Fakultät für Medizin

Institut für Pharmakologie und Toxikologie

# Role of the Cullin-RING E3 ubiquitin ligase 7 in oncogenic transformation by simian virus 40 large T-antigen

**Thomas Hartmann**

Vollständiger Abdruck der von der Fakultät für Medizin der Technischen Universität München zur Erlangung des akademischen Grades eines Doktor der Naturwissenschaften (Dr. rer. nat.) genehmigten Dissertation.

| | |
|---|---|
| Vorsitzender: | Univ.-Prof. Dr. Thomas Misgeld |
| Prüfer der Dissertation: | |
| | 1. Univ.-Prof. Dr. Dr. Stefan Engelhardt |
| | 2. Univ.-Prof. Dr. Claus Schwechheimer |

Die Dissertation wurde am 19. Februar 2014 bei der Technischen Universität München eingereicht und durch die Fakultät für Medizin am 04. Juni 2014 angenommen.

# Table of contents

# 1 Introduction

Simian virus 40 (SV40) is a prototype member of the *Polyomaviridae* family and its study led to many important discoveries in and understanding of cell biology, such as discovery of the tumor suppressor p53 (1) and insights into the structure and function of the retinoblastoma tumor suppressor pRB (2). The name *Polyomaviridae* relates to the oncogenic potential of this viral family and derives from the Greek *poly*, meaning many, and *oma*, denoting cancer (3). SV40 was first discovered in 1960 as a vaculating virus in rhesus monkey kidney cell cultures (4). Until today, nine human polyomaviruses are identified and four of these, BK polyomavirus (BKV), JC polyomavirus (JCV), Trichodysplasia spinulosa-associated polyomavirus (TSV) and Merkel cell polyomavirus (MCV) have been linked to disease (5).

The *Polyomaviridae* are characterized by small icosahedral virions of 40-45 nm diameter and by a single circular double-stranded DNA genome of about 5 kb. The genome consists of three parts: a regulatory region, containing a unique origin of replication (*ori*) and the promoters for the early and late region; the early region, encoding the proteins expressed before the onset of DNA replication; and the late region, encoding the late structural proteins (Fig. 1) (6). Alternative splicing of the early transcript results in 2-5 related but distinct proteins referred to as tumor (T)-antigens because they interfere with the cell cycle regulation and are involved in cellular transformation (7). The T-antigens also drive the activation of the late region, which encodes three structural viral proteins (VP1-3) and as well additional proteins (6).

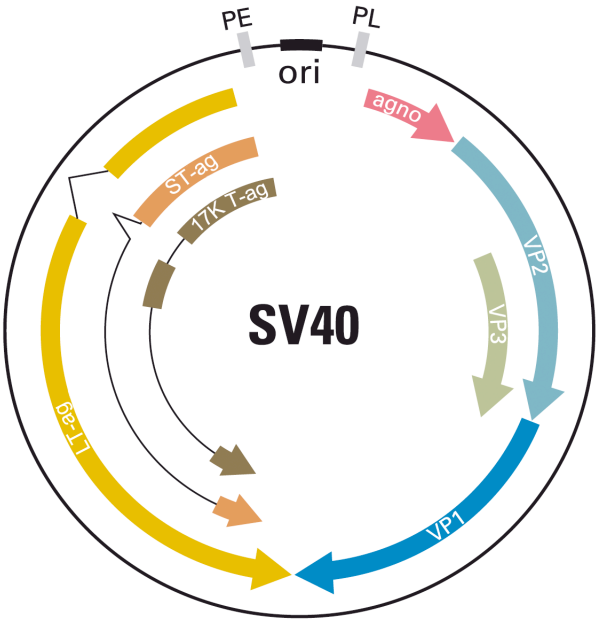


**Fig. 1. SV40 genome organization.** Schematic representation of the proteins encoded by the SV40 genome. PE, early promoter; PL, late promoter; ori, origin of replication; LT-ag, large T-antigen; ST-ag, small T-antigen; 17K T-ag, 17K T-antigen; agno, agnoprotein; VP1-3, viral capsid proteins 1-3 (modified from (8)).

The genome of SV40 consists of 5243 bp and encodes seven proteins, three from the early region and four from the late region (9, 10). The viral early region encodes the large T-antigen (LT-antigen), small T-antigen (ST-antigen) and 17K T-antigen. The late region of the genome encodes the viral capsid proteins (VP1-3) and the viral agnoprotein (Fig. 1).

While the expression of LT-antigen alone, without any other SV40 protein, is sufficient for the transformation of several cell lines (11, 12), ST-antigen alone cannot transform cells but can cooperate with LT-antigen to fully transform cells especially when LT-antigen expression is limiting (13). The main target of ST-antigen is the serine-threonine protein phosphatase A (PP2A) (14–16).

## 1.1 LT-antigen of SV40

SV40 LT-antigen is a multifunctional protein that orchestrates viral DNA replication and transcription, is able to immortalize and transform many cell types in culture and induce neoplasia in rodents.

### 1.1.1 Domain organization and interaction partners of LT-antigen

LT-antigen consists of 708 amino acids (aa) and contains four conserved domains. These four domains of LT-antigen are the N-terminal J domain, the origin binding domain (OBD), the zinc (Zn)-binding domain and the DNA helicase/ATPase domain. In addition to this four well-folded domains the protein consists of two large flexible and disordered regions, one linking the J domain and the OBD and one at the C-terminus of LT-antigen (Fig. 2) (5). Both, the four well-folded domains and the flexible regions, contain binding regions for key proteins involved in cellular transformation and viral DNA replication (Table 1).

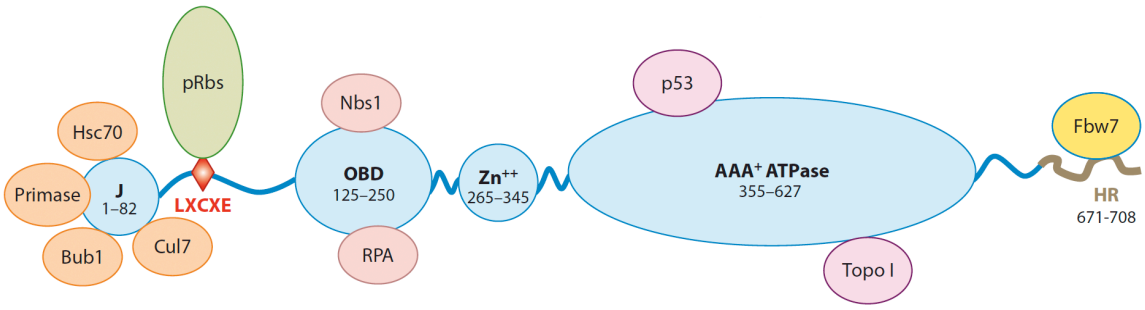


**Fig. 2. Domain organization and binding partners of LT-antigen.** Schematic representation of SV40 LT-antigen domains and their binding partners. Amino acid (aa) regions of each domain are indicated. J, J domain; Primase, polymerase α primase; pRBs, retinoblastoma protein family; CUL7, Cullin 7; OBD, origin binding domain; RPA, replication protein A; $Zn^{++}$, Zinc binding domain; $AAA^{+}$ ATPase, DNA helicase/ATPase domain; Topo I, topoisomerase I; HR, host range domain; Fbw7, F-box and WD40 repeat-containing 7 (modified from (5)).

### The J domain

The N-terminal J domain of LT-antigen contains a structural conserved DnaJ motive present in the DnaJ family of molecular chaperones (17). It binds to polymerase α primase involved in viral DNA replication (18) and is implicated in LT-antigen mediated transformation by promoting the release of E2F transcription factors from pRB-family members (19, 20) involving HSC70 binding and activation of its ATPase activity (21).

### The origin binding domain (OBD)

The OBD binds to the viral *ori* and is essential for the initiation of viral DNA replication. Further binding partners of the OBD include the replication protein A (RPA), essential for viral DNA replication (22) and the MRE11, RAD50 and NBS1 (MRN) complex (23, 24), involved in repair of double-strand DNA breaks by homologous recombination.

**Table 1: LT-antigen domains, interaction partners and involvement in viral DNA replication or oncogenic transformation by LT-antigen.**

| Domain | Binding partner | Involved in |
|---|---|---|
| J domain | polymerase α primase | viral DNA replication (18) |
| | HSC70 | Transformation (19, 20) |
| linker region in-between J domain and OBD | CUL7 | Transformation (25, 26) |
| | pRB-family | Transformation (27) |
| | BUB1 | Transformation (28) |
| OBD | *ori* | viral DNA replication |
| | RPA | viral DNA replication (22) |
| | MRN complex | viral DNA replication (23, 24) |
| Zn-binding domain | LT-antigen (hexamerization) | viral DNA replication |
| DNA helicase/ATPase domain | topoisomerase I | viral DNA replication (22) |
| | p53 | Transformation (29, 30) |
| C-terminus | Fbw7 | Transformation (31) |

### The flexible linker in-between J domain and OBD

The flexible linker in-between J domain and OBD includes binding sites for Cullin 7 (CUL7), the spindle checkpoint kinase BUB1 and the LXCXE motif for binding of the pRB-family of proteins. While binding of LT-antigen to BUB1 seems to be involved in the induction of DNA damage response (DDR) by LT-antigen (28), CUL7 and pRB-family binding are involved in cellular transformation (25–27).

**The Zn-binding domain and DNA helicase/ATPase domain**

The Zn-binding domain mediates the oligomerization of LT-antigen to its hexameric state and together with the DNA helicase/ATPase domain builds the core for the DNA helicase activity. The DNA helicase/ATPase domain also interacts with topoisomerase I (22) and binds and inactivates the p53 tumor suppressor (1).

**The C-terminal region of LT-antigen**

The C-terminus of LT-antigen includes the host range domain (HR), which harbors a binding site for F-box and WD40 repeat domain containing protein 7 (Fbw7). Fbw7 binding is dependent on phosphorylation of threonine 701 on LT-antigen and interferes with the degradation of Cyclin E1 by the Cullin1$^{Fbxw7}$ E3 ligase complex (31).

### 1.1.2 Functions of LT-antigen

LT-antigen is involved in organization of the viral DNA replication and is able to induce cellular transformation (Table 1).

**Viral DNA replication**

LT-antigen is the key protein for organizing the viral DNA replication during the productive life cycle of SV40. LT-antigen binding to the *ori*, binding of multiple host cell replication factors and association into double hexamers that possess helicase activity are essential for viral DNA replication. Regulation of viral DNA replication by LT-antigen seems to be due to different posttranslational modifications of LT-antigen, especially phosphorylation. Several LT-antigen phosphorylation mutants showed to be deficient in viral DNA replication but still retained cell transformation activity (32). After binding of the OBD to the *ori* the Zn-binding domain mediates the assembly of LT-antigen monomers to the double hexameric state (33). In the double hexameric state the helicase domain is in its active form and can melt the origin of replication and further unwind the DNA during replication. The cellular interaction partners needed for viral DNA replication have been identified and SV40 replication successfully reconstituted *in vitro* (22). The study of SV40 DNA replication provided important insights on the understanding of eukaryotic DNA replication.

**Oncogenic transformation by SV40 LT-antigen**

The current understanding of oncogenic transformation by LT-antigen is based on the inactivation of two essential tumor suppressors of the cell, the pRB-family of proteins and p53 (34).

The pRB-family consists of the retinoblastoma proteins pRB, p107 and p130 that negatively regulate cell proliferation via binding and inhibition of the E2F family of transcription factors

(35, 36). The E2F transcription factors regulate the expression of genes required for entry into and progression through the cell cycle. In the normal cell cycle progression Cycline dependent kinases (Cdk) phosphorylate and inactivate the pRB proteins resulting in release of the E2F transcription factors. LT-antigen binds and inactivates all three pRB proteins directly via its LXCXE motif (27). Activation of the HSC70 ATPase activity by the J domain also contributes to the release of E2F transcription factors of the pRB-family proteins and both an intact LXCXE domain and functional J domain are required for transformation.

p53 is a sequence specific transcription factor that is activated in response to different cellular stresses and induces cell cycle arrest or apoptosis (37). The levels of p53 are tightly regulated and kept at low levels by mouse double minute 2 homolog (MDM2), an E3 ligase that ubiquitinates p53 and marks it for proteasomal degradation (38, 39). Activation of p53 by cellular stresses results in phosphorylation and subsequent acetylation of p53, thereby inhibition of MDM2 binding and increase of p53 levels, leading to initiation of p53-dependent transcription (40). LT-antigen inhibition of p53 function is essential for the transformation, LT-antigen mutants unable to bind p53 are transformation deficient (29, 30).

In addition to binding and inactivation of the two main tumor suppressors of the cell, it was shown that the association of LT-antigen with CUL7 is a prerequisite for LT-antigen induced transformation. CUL7 is the scaffold protein of the Cullin-RING E3 ubiquitin ligase 7 (CRL7), a E3 ligase in the ubiquitin-proteasome system, and was first reported as an LT-antigen associated protein (41, 42). CUL7 binding deficient mutants of LT-antigen, that still retain the pRB and p53 binding sites were shown to be transformation deficient (25, 26).

## 1.2 The ubiquitin-proteasome system (UPS)

For ubiquitin-mediated degradation of substrate proteins by the UPS proteins are first covalently marked by attachment of a chain of ubiquitin molecules and then the modified proteins are recognized in a second step by the 26S proteasome, which promotes the proteolysis of the substrate (Fig. 3). The attachment of an ubiquitin chain to the substrate protein, is carried out by a three-tiered enzymatic cascade (43, 44), first the chemical inert ubiquitin is activated in an ATP-dependent reaction by an E1 ubiquitin-activating enzyme and transferred to an E2 conjugating enzyme. The ubiquitin loaded E2 then in concert with an E3 ubiquitin ligase promotes the transfer of ubiquitin to the substrate protein, resulting in mono-, multi- or polyubiquitination of the substrate. The different ubiquitination patterns have multifaceted functions, while mono- and multiubiquitination in general result in non-proteolytic outcomes (45, 46), polyubiquitination is often but not exclusively linked to

degradation of the target protein by the 26S proteasome and depends on the chain structure (47).

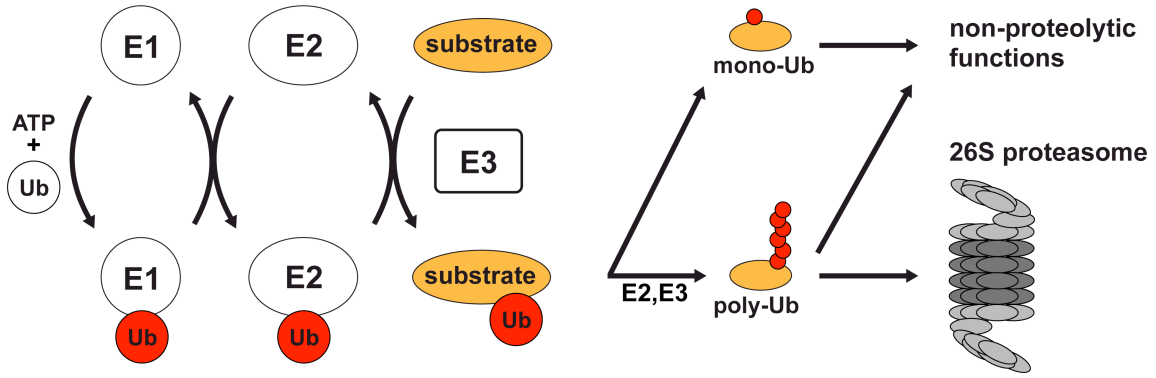


**Fig. 3. The ubiquitin-proteasome system (UPS).** Schematic representation of the UPS. In a three-tiered enzymatic cascade ubiquitin (Ub) is transferred to the substrate protein, resulting in mono-, multi- (not shown) or polyubiquitination. The type of ubiquitination determines if the substrate is degraded by the 26S proteasome or has other non-proteolytic functions (modified from (48)).

For instance Lys48-linked polyubiquitin chains are the canonical signal for proteasomal degradation, while Lys63-linked chains have non-proteolytic functions in cell signaling (45, 47).

## 1.3 E3 ubiquitin ligases

The substrate specificity of the UPS is on of its key futures and is mainly achieved by the E3 ubiquitin ligases. While there are only two E1 enzymes and around 37 E2 enzymes encoded in the human genome, more than 600 E3 ligases are encoded (47). There are three major classes of E3 ligases, the HECT (homologous to E6-associated protein C-terminus), the RING (Really Interesting New Gene)-finger and the U-box E3s (49).

HECT E3 ligases are characterized by a 350 aa HECT domain and by formation of an ubiquitin-E3 intermediate before covalent attachment of ubiquitin to the substrate. In contrast RING and U-box E3s act as scaffolds and promote the direct transfer of ubiquitin from the E2 conjugating enzyme to the substrate protein by bringing them in close proximity (49). RING E3 ligases are characterized by the RING-finger domain, a cysteine/histidine-rich, zinc-chelating domain involved in E2 binding (50). U-box E3 ligases are characterized by the U-box, a 74 aa domain that is structurally similar to the RING-finger domain but lacks the metal chelating residues (51). With hundreds of RING-containing proteins encoded in the mammalian genome RING-finger E3 ligases potentially represent the largest class of E3 ligases but in most cases prove of E3 ligase activity *in vivo* is missing (52).

RING-finger E3 ligases can be further divided into two classes, the first consists of single molecule RING E3 ligases that contain the substrate-binding site and the RING-finger domain on the same polypeptide, the second group is composed of the multi-subunit Cullin-RING E3 ubiquitin ligases (CRLs) (53, 54). CRLs are composed of a central Cullin (CUL) scaffold protein that together with the RING subunit ROC1 or ROC2 builds the catalytic core of the E3 ligase. A Cullin-homology (CH) domain that is essential for binding the RING-finger subunit characterizes all Cullins. The mammalian Cullin family consists of eight members, seven Cullins (CUL1, CUL2, CUL3, CUL4A, CUL4B, CUL5 and CUL7) and in addition the closely related PARC (p53-associated parkin-like cytoplasmatic protein) (55). CUL1 to CUL5 share a general structure, with a long stalk-like N-terminal domain consisting of three cullin repeats (CR1 to CR3) involved in binding of the substrate adaptor proteins and a globular carboxy-terminal domain that harbors the CH domain (56). CUL7 and PARC form atypical CRLs, they also share the characteristic CH domain at their C-terminal regions but have distinct N-terminal domains containing a CPH domain, a domain conserved in CUL7, PARC and HERC2, involved in p53 binding and a DOC domain of unknown function (Fig. 4). In addition all Cullins have a verified or, based on sequence analysis, predicted neddylation site following the CH domain (57).

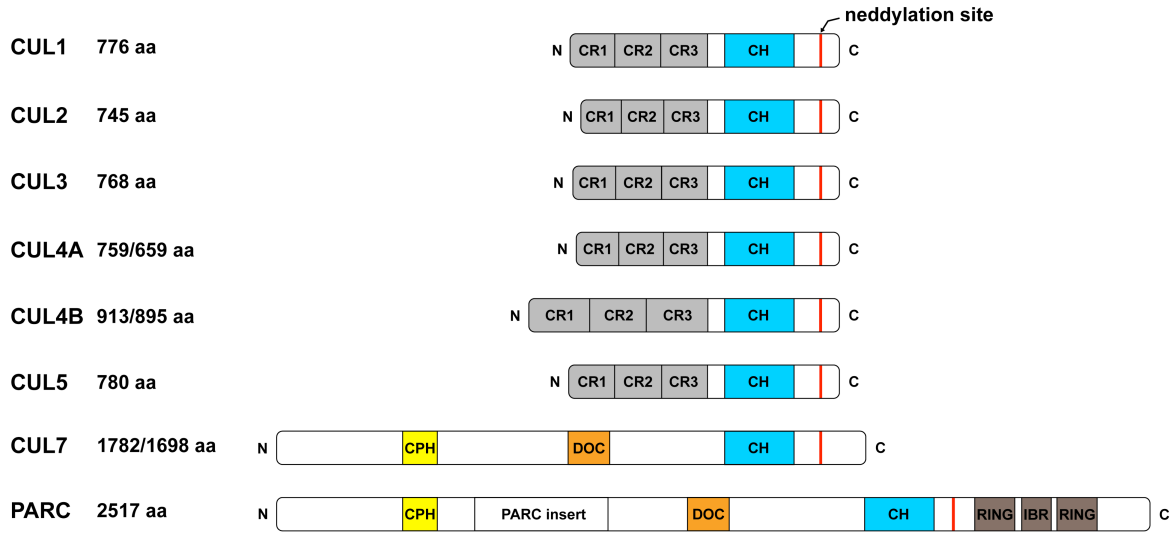


**Fig. 4. Domain organization of the different Cullin proteins.** Schematic representation of the domains conserved in Cullin proteins. CR1-3, cullin repeats 1-3; CH, cullin homology domain; CPH, domain conserved in CUL7, PARC and HERC2; RING, Really Interesting New Gene; IBR, in between RING (modified from (48)).

CRL are composed of the CRL catalytic core (Cullin protein and RING-finger protein) and a substrate recognition complex consisting of an adaptor protein and a substrate recognition protein (Fig. 5A). The full-assembled ligase positions the substrate and the ubiquitin loaded E2 in close proximity and promotes direct ubiquitin transfer from E2 to the substrate (58). The high modularity of the CRLs is achieved by different adaptor proteins used by different

Cullin proteins and a multitude of substrate recognition proteins specific for the different ligase complexes (58). For example the prototypical CRL complex based on CUL1, also referred to as SCF (Skp1, CUL1, F-box) complex, is based on the adapter protein S-phase kinase-associated protein 1 (Skp1) and the F-box protein family of substrate receptors. Substrate-recognition molecules of other CRLs include VHL-box, SOCS-box and DCAF protein families each containing distinct motifs that are recognized by an adaptor specific for the cognate Cullin. CRL3 complexes miss an adaptor protein and substrate targeting is mediated via Bric-a-brac, Tramtrack, Broad-complex (BTB) domain proteins (Fig. 5B).

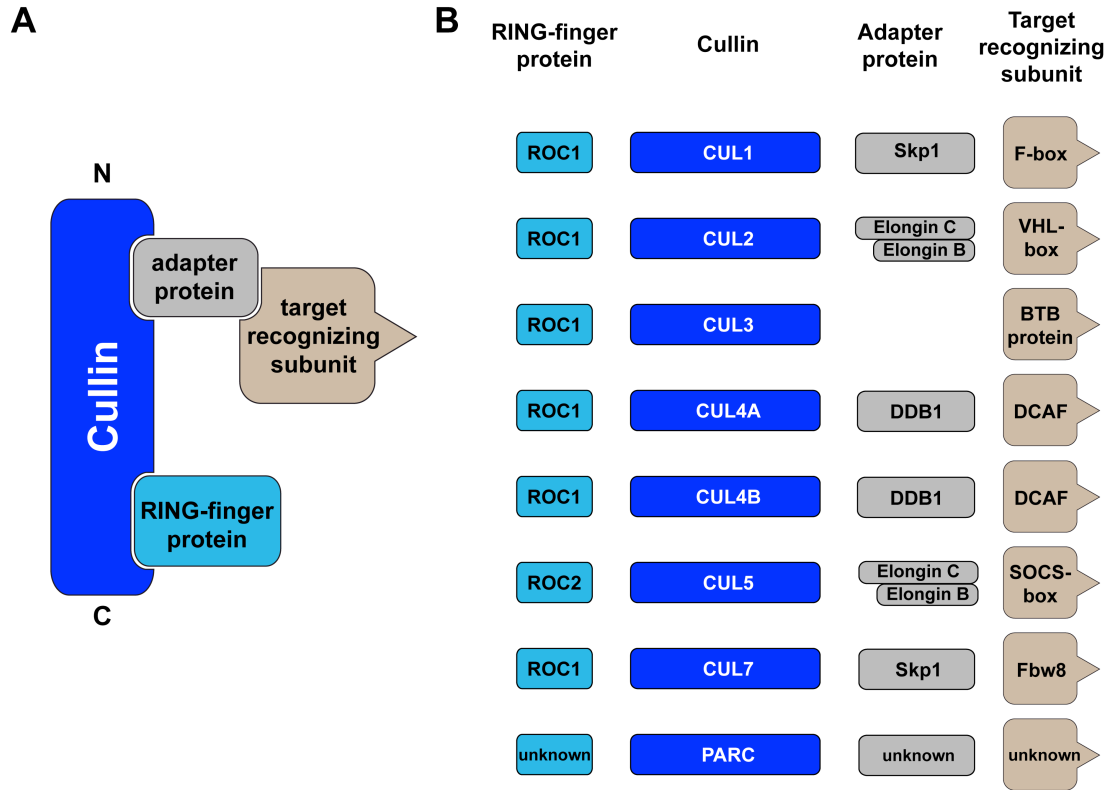


**Fig. 5. Composition of Cullin-RING E3 ubiquitin ligases.** Schematic representation of the modular composition of Cullin-RING E3 ubiquitin ligases (CRLs). **A** CRLs are in general composed of a Cullin scaffold protein that via its amino terminus tethers a substrate-recognition complex, mainly composed of a adapter protein and the target recognition protein, and at its C-terminus a RING-finger protein. **B** Specific composition of the different CRLs. Skp1, S-phase kinase-associated protein 1; VHL-box, von Hippel-Lindau box; BTB, Bric-a-brac, Tramtrack, Broad-complex; DCAF, DDB1-CUL4 associated factor; DDB1, DNA damage-binding protein 1; Fbw8, F-box and WD40 repeat domain containing protein 8; SOCS, Suppressor of cytokine signaling (modified from (48)).

CRLs are involved in a multitude of cellular processes including cell-cycle control, DNA replication and development, making tight control of CRL activity crucial for maintaining cellular integrity. Covalent attachment of the small ubiquitin-like protein NEDD8, termed neddylation, positively regulates CRL activity by inducing conformational rearrangements that increase the flexibility of the Cullin bound RING-finger protein and allows it to adopt orientations that favor ubiquitin transfer from the bound E2 enzyme to the substrate (59, 60).

The COP9 Signalosome (CSN) hydrolyzes the Cullin-NEDD8 conjugates and reverses neddylation (61). Another negative regulator of CRLs is CAND1 (Cullin-associated and neddylation-dissociated protein 1), it was shown to bind CUL1 in a head-to-tail fashion, thereby interfering with Skp1 binding and neddylation (62). It was also observed that the F-box proteins are a rate-limiting component of CRL-mediated degradation (63). This may be due to low expression levels or the short half-life of many F-box proteins that involves auto-ubiquitination of the F-box proteins by the E3 ligase (64). Beside the regulation of the CRL itself also the recognition of the target protein by the E3 ligase is highly regulated. In many cases posttranslational modifications like phosphorylation are necessary for the recognition of the target protein by the substrate recognition protein. The mechanism of substrate recognition by F-box proteins has been extensively studied and was recently reviewed by Skaar et al. (65).

## 1.4 Cullin-RING E3 ubiquitin ligase 7

The scaffold protein of the Cullin-RING E3 ubiquitin ligase 7 (CRL7) is CUL7, which was initially found as SV40 LT-antigen associated protein in screens for LT-antigen interaction partners (41, 42). CUL7 was later identified to form a atypical CRL due to its size and additional domains compared to other Cullins (66) (Fig. 4). CRL7 is composed of the scaffold protein CUL7, the RING-finger protein ROC1 and the substrate adaptor Skp1. In contrast to the SCF complex, which via Skp1 interacts with a multitude of F-box proteins, CRL7 assembles only with Fbw8 (Fig. 5B).

### 1.4.1 CUL7 binding partners

In addition to the ligase subunits and LT-antigen, CUL7 interacts directly with p53, obscurin-like protein 1 (OBSL-1), Glomulin and PARC (67–71) (Table 2).

**Table 2: CUL7 binding partners, binding domains and functions.**

| Binding partner | Domain | Function |
|---|---|---|
| Glomulin (69) | C-terminus/ROC1 | inhibition of E2 binding |
| LT-antigen (41, 42) | unkown | implication in LT-antigen mediated transformation |
| OBSL-1 (70) | C-terminus | localizes CUL7 at the Golgi apparatus; involved in GRASP65 degradation/Golgi morphogenesis |
| p53 (67) | CPH domain | unkown |
| PARC (71) | unkown | dimerization of PARC and CUL7, functional relevance unclear |
| ROC1 (66) | CH domain | E2 binding |
| Skp1 (66) | N-terminal region | Fbw8 binding |

While p53 interacts with the CPH domain in the N-terminal part of CUL7, OBSL-1 and Glomulin interact with the C-terminal region of CUL7. The binding region of PARC has not been determined yet. Binding of CUL7 to p53 has been proposed to sequester p53 into the cytoplasm or to act as ubiquitin ligase for p53 degradation but subsequent studies have found no role for CUL7 in this processes and present the option that p53 might modify CRL7 function (71, 72). OBSL-1, a cytoskeletal adaptor protein, was shown to be a critical regulator of CRL7 in the control of Golgi morphogenesis involving Golgi reassembly-stacking protein 1 (GRASP65) degradation (70). Glomulin not only interacts with CUL7 but with all ROC1 containing Cullins via interaction of the RING-finger domain of ROC1 (73). Glomulin interaction with the SCF complex inhibits SCF-mediated ubiquitination by blocking the E2-interacting surface of ROC1 (74). CUL7 and PARC were the first example of Cullin dimerization (71). CUL7 and PARC containing complexes were shown to exhibit ubiquitin ligase activity but the functional relevance of these dimers is still not clear (75).

### 1.4.2 CRL7 substrates

To date there are six identified substrates for the CRL7 (Table 3): cyclin D1 (76), the MRN complex (24), GRASP65 (70), TBC1 Domain Family Member 3 (TBC1D3) (77), Hematopoietic Progenitor Kinase1 (HPK1) (78) and the insulin receptor substrate 1 (IRS1) (79). IRS1 was recently confirmed as CRL7 target by Zhang et al. showing decreased IRS1 protein level upon Fbw8 up-regulation in mouse embryonic fibroblasts (MEFs) of liver kinase 1 (LKB1) deficient mice that was prevented by siRNA depletion of Fbw8 (80).

**Table 3: CUL7 substrates.**

| Substrate | Substrate adaptor | Function |
|---|---|---|
| Cyclin D1 (76) | Skp1-Fbw8 | cell cycle regulation |
| GRASP65 (70) | Skp1-Fbw8 | Golgi morphology |
| HPK1 (78) | Skp1-Fbw8 | mammalian Ste20-like serine/threonine kinase |
| IRS1 (79) | Skp1-Fbw8 | central mediator in insulin and IGF-1 signaling |
| MRN complex (24) | Skp1-Fbw8 | DNA damage repair |
| TBC1D3 (77) | Skp1-Fbw8 | hominoid-specific oncogene |

### 1.4.3 Biological significance of CRL7

Genetic studies documented a pivotal growth-regulatory role of CRL7. Knockout mice with a target disruption of the *cul7* (*cul7*$^{-/-}$ mice) (69) or *fbw8* (81) gene exhibit intrauterine growth retardation and neonatal lethality. Further, dysregulation of CRL7 by *CUL7* germline

mutations was found in patients with 3-M syndrome (82), characterized by pre- and postnatal growth retardations in humans and as well in Yakuts dwarfism syndrome (83).

CRL7 has also been implicated in the regulation of the insulin and insulin like growth factor 1 (IGF-1) signaling pathways by IRS1 degradation. IRS1 is a central component in insulin and IGF-1 signaling. Upon receptor activation and phosphorylation IRS1 is recruited to the receptor and phosphorylated on several tyrosine residues, mediating receptor activation to the phosphatidylinositide 3-kinase (PI3K)/AKT and extracellular signal-regulated kinase (Erk) mitogen-activated protein kinase (MAPK) signaling pathways (84). A negative feedback loop via mTORC1/S6K1 phosphorylates serine residues on IRS1, generating an phosphodegradation motif for CRL7 mediated ubiquitination and degradation of IRS1 (79, 85, 86). In addition to the mTORC1/S6K1 negative feedback loop, mTORC2-mediated phosphorylation of Fbw8 resulted in increased stability of the F-box protein, promoting IRS1 degradation (85, 87). A more recent study showed that TBC1D3 is also involved in controlling IRS1 stability. TBC1D3 expression reduced IRS1 serine phosphorylation levels, resulting in delayed ubiquitination and degradation of IRS1 and increased AKT signaling (88). In addition, *cul7*$^{-/-}$ MEFs display increased levels of IRS1 and activation of the downstream signaling pathways PI3K/AKT and Erk MAPK (79).

A transgenic mouse model with over-expression of IRS1 in the mammary gland displays progressive mammary hyperplasia, tumorigenesis and metastasis (89). Also dysregulation or mutations in the IRS1 downstream pathways PI3K/AKT and Erk MAPK are often linked to tumorigenesis and cancer (90–99). Increased IRS1 protein levels and constitutive phosphorylation of IRS1 was also observed in human cancers (100–102).

**CRL7 and oncogenic transformation by SV40 LT-antigen**

The CRL7 scaffold protein CUL7 has been implicated in the oncogenic transformation by LT-antigen. A CUL7 binding deficient mutant of LT-antigen, that retained the ability to bind p53 and pRB was shown to be transformation deficient (25, 26), showing that CUL7 binding is essential for SV40 LT-antigen transformation.

In addition, Baserga and co-workers investigated the involvement of the IGF-1 receptor (IGF-1R) and IRS1 in the transformation by LT-antigen. They were able to show that cells lacking the IGF-1R cannot be transformed by LT-antigen (103, 104) and that an active IRS1/PI3K signaling via tyrosine phosphorylated IRS1 is required (105). The transformational phenotype could be rescued by either IGF-1R or IRS1 co-expression (104, 106, 107). Further, LT-antigen translocates IRS1 to the nucleus and activates ribosomal DNA, c-myc and cyclin D1 promoters which may contribute to malignant transformation (108, 109).

## 1.5 Aim of this study

The aim of this study was to assess the role of CRL7 in oncogenic transformation by SV40 LT-antigen. The objectives were:

- to investigate the effect of SV40 LT-antigen expression on CRL7 E3 ligase mediated IRS1 degradation,
- to analyze the SV40 LT-antigen effect on IRS1 downstream signaling pathways PI3K/AKT and Erk MAPK, and
- to elucidate the molecular mechanisms of the proposed CRL7 inhibition by LT-antigen.

# 2 Materials and Methods

## 2.1 Chemicals

All chemicals were purchased at AppliChem (Darmstadt, Germany), Carl Roth (Karlsruhe, Germany) or Sigma Aldrich (Taufkirchen, Germany) unless otherwise noted. Protected brand and trade names are not indicated in this work.

## 2.2 Antibodies

| Antibody | Reactivity | Host | Dilution | Company |
|---|---|---|---|---|
| Alexa Fluor 488 Goat Anti-Mouse IgG (H+L) | mouse | goat | IF: 1:400 | Invitrogen |
| AKT | human, mouse | rabbit | WB: 1:1000 | Cell Signaling |
| Alexa Fluor 594 Goat Anti-Rabbit IgG (H+L) | rabbit | goat | IF: 1:400 | Invitrogen |
| c-myc (9E10) | human, mouse | mouse | WB: 1:500 | Santa Cruz Biotechnology |
| CUL7 | human | rabbit | WB: 1:1000 | Sigma Aldrich |
| CUL7 (Ab38) | human, mouse | mouse | WB: 1:1000 | Sigma Aldrich |
| flag (M2) | flag epitope | mouse | WB: 1:1000 | Sigma Aldrich |
| GST | glutathione S-transferase | mouse | WB 1:1000 | Santa Cruz |
| HA.11 Clone 16B12 | HA epitope | mouse | WB: 1:1000 | HiSS Diagnostics |
| HRP-anti-mouse | mouse | horse | WB: 1:10.000 | Cell Signaling |
| HRP-anti-rabbit | rabbit | goat | WB: 1:10.000 | Cell Signaling |
| HSP 90α/β (F-8) | human, mouse | mouse | WB: 1:10.000 | Santa Cruz Biotechnology |
| IRS1 | human, mouse | rabbit | WB: 1:1000 | Millipore |
| p44/42 MAPK (Erk1/2) (L34F12) | human, mouse | mouse | WB: 1:1000 | Cell Signaling |
| Phospho-AKT (Ser473) | human, mouse | rabbit | WB: 1:1000 | Cell Signaling |
| Phospho-p44/42 MAPK (Erk1/2) (Thr202/Tyr204) | human, mouse | rabbit | IF: 1:50<br>WB 1:1000 | Cell Signaling |
| SV40 T Ag (Pab 416) | LT-antigen SV40 | mouse | WB: 1:1000 | Calbiochem |
| SV40 T Ag (Pab 419) | LT-antigen SV40 | mouse | WB: 1:1000 | Santa Cruz Biotechnology |

| | | | | |
|---|---|---|---|---|
| SV40 T Ag (v-300) | LT-antigen SV40 | rabbit | IF: 1:50<br>IHC: 1:50 | Santa Cruz Biotechnology |
| V5 | V5 epitope | mouse | WB: 1:5000 | Invitrogen |

## 2.3 Oligonucleotides

All oligonucleotides used in this work were purchased at MWG Biotech (Ebersberg, Germany) or Sigma Aldrich. Stock solutions of 100 µM were prepared in double distilled (dd) $H_2O$ and stored at -20°C. Working solutions of 20 µM were prepared for all experiments.

| Primer | Sequence (5´→3´) | Product |
|---|---|---|
| pcDNA3.1-EcoRI-LT-ag fwd | AAA GAA TTC ATG GAT AAA GTT TTA AAC AGA GAG GAA TCT TTG | EcoRI-LT-ag-NotI/ EcoRI-ΔLT-ag-NotI |
| pcDNA3.1-LT-ag-NotI rev | TTT GCG GCC GCT TAT GTT TCA GGT TCA GGG GGA GG | |
| pcDNA3.1-EcoRI-LT-ag fwd | AAA GAA TTC ATG GAT AAA GTT TTA AAC AGA GAG GAA TCT TTG | EcoRI-LT-ag-V5-NotI/EcoRI-ΔLT-V5-ag-NotI |
| pcDNA3.1-LT-ag-NotI-V5 rev | TTT GCG GCC GCT TAC GTA GAA TCG AGA CCG AGG AGA GGG TTA GGG ATA GGC TTA CCT CCT GTT TCA GGT TCA GGG GGA GGT G | |
| pcDNA3.1-EcoRI-LT-ag fwd | AAA GAA TTC ATG GAT AAA GTT TTA AAC AGA GAG GAA TCT TTG | EcoRI-LT-ag-HA-NotI/ EcoRI-ΔLT-HA-ag-NotI |
| pcDNA3.1-LT-ag-NotI-HA rev | TTT GCG GCC GCT TAA GCG TAA TCT GGA ACA TCG TAT GGG TAT GCT GTT TCA GGT TCA G | |
| pBABE-BamHI-LT-ag fwd | AAA GGA TCC ATG GAT AAA GTT TTA AAC AGA GAG GAA TCT TTG | BamHI-LT-ag-EcoRI/ BamHI-ΔLT-ag-EcoRI |
| pBABE-EcoRI-LT-ag rev | TTT GAA TTC TTA TGT TTC AGG TTC AGG GGG AGG | |
| qPCR hGAPDH fwd | GAT CAT CAG CAA TGC CTC CT | 140 bp of human *GAPDH* gene |
| qPCR hGAPDH rev | GGG CCA TCC ACA GTC TTC T | |
| qPCR V5-IRS1 fwd | TAA CCC TCT CCT CGG TCT CG | 128bp of V5-IRS1 cDNA |
| qPCR V5-IRS1 rev | GCG CAC GTC CGA GAA GCC AT | |
| qPCR 18S fwd | TCG AGG CCC TGT AAT TGG AAT | 61bp of 18S rRNA |
| qPCR 18S rev | CCC TCC AAT GGA TCC TCG TTA | |
| qPCR c-fos fwd | AAC CAC AGG GAA AGG AGA CC | 60bp of c-fos cDNA |
| qPCR c-fos rev | ATG GTG CCT GCG TGA TAC T | |

## 2.4 Plasmids

| Vector | Insert | Reference |
|---|---|---|
| pcDNA3.1 | EV | Invitrogen |
| pcDNA3.1 | large T-antigen | generated in this work |
| pcDNA3.1 | Δ69-83 large T-antigen | generated in this work |
| pcDNA3.1 | HA-tagged large T-antigen | generated in this work |
| pcDNA3.1 | HA-tagged Δ69-83 large T-antigen | generated in this work |
| pcDNA3.1 | V5-tagged large T-antigen | generated in this work |
| pcDNA3.1 | V5-tagged Δ69-83 large T-antigen | generated in this work |
| pBABE-puro | EV | Addgene plasmid 1764 |
| pBABE-puro | large T-antigen | generated in this work |
| pBABE-puro | Δ69-83 large T-antigen | generated in this work |
| pCR3.1 | myc-Fbw8 | Dias et al. 2002 (66) |
| pCR3.1 | flag-CUL7 | Dias et al. 2002 (66) |
| pcDNA3.1 | V5-IRS1 | Xu et al. 2008 (79) |
| pcDNA3 | HA CUL7 | Litterman et al. 2011 (70) |
| pcDNA3 | HA ΔN CUL7 | Litterman et al. 2011 (70) |
| pcDNA3 | HA ΔDOC CUL7 | Litterman et al. 2011 (70) |
| pcDNA3 | HA ΔCUL CUL7 | Litterman et al. 2011 (70) |
| pcDNA3 | HA ΔC CUL7 | Litterman et al. 2011 (70) |

## 2.5 Small interfering RNA (siRNA)

Synthetic siRNA-duplexes with 3´ dTdT overhangs were purchased at Sigma Aldrich:

| Target mRNA | Sequence |
|---|---|
| Cullin 7 siRNA 1 | 5´-GAC UUU GUG CCA CGC UAC U-3´ |
| Cullin 7 siRNA 2 | 5´-CAA UAC CUA UGC UUU GUA U-3´ |
| Cullin 7 siRNA 3 | 5´-GUU GAG UAG UCC UGA UUA U-3´ |
| scramble control | siRNA Universal Negative Control 1 |

## 2.6 Enzymes

| | |
|---|---|
| AccuPrime *Pfx* DNA Polymerase | Invitrogen (Karlsruhe, Germany) |
| Alkaline Phosphatase | New England Biolabs (NEB, Frankfurt am Main, Germany) |
| Antarctic Phosphatase | NEB |
| Benzonase | Merck (Darmstadt, Germany) |
| DNAse I | Qiagen (Hilden, Germany) |
| Platinum Taq DNA Polymerase | Invitrogen |
| Proteinase K | AppliChem |
| Restrictions endonucleases | NEB |
| Reverse Transcriptase | Invitrogen |
| T4 DNA Ligase | NEB |
| Taq DNA Polymerase | GenScript (Piscataway, USA) |
| Trypsin | GIBCO (Karlsruhe, Germany) |

## 2.7 Bacteria

| Strain | Genotype | Source |
|---|---|---|
| E. coli DH10B | F– mcrA Δ(mrr-hsdRMS-mcrBC) Φ80lacZΔM15 ΔlacX74 recA1 endA1 araD139 Δ(ara leu) 7697 galU galK rpsL nupG λ– | Invitrogen |

## 2.8 Eukaryotic Cell lines

| Name | Description | Source |
|---|---|---|
| HEK293 cells | Human embryonic kidney cell line | Invitrogen |
| MCF7 cells | Human breast cancer cell line | Prof. Dr. Pan, Mount Sinai School of Medicine, Icahn Medical Institute, Dept. of Oncological Sciences, New York, USA |
| Phoenix-AMPHO cells | based on HEK293 cells second-generation retrovirus producer cell line for the generation of helper-free amphotropic retroviruses | ATCC (Wesel, Germany) |
| U2-OS cells | Human bone osteosarcoma cell line | kind gift of Prof. Dr. Holm, Experimentele Onkologie, Klinikum rechts der Isar, Germany |

## 2.9 Mouse lines

| Name | Description | Source |
|---|---|---|
| CEA424/T-antigen transgenic mice | mouse line over-expressing the large T-antigen under the control of 424 bp of the carcinoembryonic antigen (CEA) | Prof. Dr. Zimmermann (110) |

## 2.10 Molecular biology

### 2.10.1 Polymerase chain reaction (PCR)

For the amplification of plasmid DNA the AccuPrime *Pfx* DNA Polymerase with 3´-5´ exonuclease activity was used.

| | | |
|---|---|---|
| Reaction mixture: | Plasmid DNA | 100 ng |
| | Primer forward | 20 pmol |
| | Primer reverse | 20 pmol |
| | AccuPrime *Pfx* reaction mix (10x) | 5 µl |
| | AccuPrime *Pfx* DNA Polymerase | 1 µl (2.5 U) |
| | $ddH_2O$ | ad 50 µl |

The amplification was carried out using the T Gradient cycler (Biometra, Göttingen, Germany) with following setup:

| PCR stage | Temperature | Time | Cycles |
|---|---|---|---|
| Initial denaturation | 95 °C | 2 min | 1 |
| Denaturation | 95 °C | 15 sec | 30 |
| Annealing | 60 °C | 30 sec | |
| Elongation | 68 °C | 2 min 30 sec (≈ 2500 bp) | |
| Final elongation | 68 °C | 5 min | 1 |

For the genotyping of mouse offspring the Taq DNA Polymerase (GenScript) was used.

| | | |
|---|---|---|
| Reaction mixture: | Isolated DNA | 1 µl |
| | Primer forward | 20 pmol |
| | Primer reverse | 20 pmol |
| | 10x PCR buffer (w/o $Mg^{2+}$) | 5 µl |
| | 50 mM MgCl2 (only Cul7 genotyping) | 1.5 µl |
| | 10 mM dNTPs | 1 µl |
| | Taq DNA Polymerase | 0.2 µl (1 U) |
| | $ddH_2O$ | ad 50 µl |

The amplification was carried out using the T Gradient cycler (Biometra) with following setup:

| PCR stage | Temperature | Time | Cycles |
|---|---|---|---|
| Initial denaturation | 95 °C | 2 min | 1 |
| Denaturation | 95 °C | 1 min | 35 |
| Annealing | 66 °C | 2 min | |
| Elongation | 72 °C | 3 min (≈3000 bp) | |
| Final elongation | 72 °C | 7 min | 1 |

### 2.10.2 RNA isolation

For the isolation of total RNA the "RNeasy Mini Kit" (Qiagen) including the optional DNAse I digestion step was used as defined by the manufacturer. The RNA was dissolved in RNase-free water and purity and concentration measured by nanodrop spectrophotometer ND 1000 (Peqlab, Erlangen Germany).

### 2.10.3 Reverse transcription

The reverse transcription for the generation of cDNA from RNA was performed using the SuperScript II Reverse Transcriptase (Invitrogen) and oligo(dT) primers (MWG Biotech).

| | | |
|---|---|---|
| Reaction mixture: | RNA | 0.5 µg |
| | 10 mM oligo(dT) primer | 2 µl |
| | RNAse free $H_2O$ | ad 11.9 µl |
| | Incubation for 10 min at 70 °C | |
| | 5x First Strand buffer | 4 µl |
| | 0.1 M DTT | 2 µl |
| | 1 mM dNTPs | 1 µl |
| | RNAse Out Recombinant Ribonuclease Inhibitor | 0.1 µl |
| | Reverse Transcriptase | 1 µl (200 U) |

The complete mixture was incubated at 42 °C for 1 hour, following heat inactivation of the enzymes (70 °C for 10 min). 30 µl RNAse free water were added for a final volume of 50 µl per sample.

### 2.10.4 Quantitative real-time PCR (qRT-PCR)

The quantitative real-time PCR is based on the classic PCR but in addition allows the quantification of a target DNA molecule. In this work the *SYBR Green* based qRT-PCR was used. *SYBR Green* (Cambrex Bioscience Rockland Inc, Rockland, USA) intercalates specifically with dsDNA and the fluorescence signal increases with every PCR cycle compared to the reference fluorophore 5-carboxyrhodamin (5-ROX; Invitrogen). The *Cycle threshold (Ct)* is defined as the cycle where the *SYBR Green* signal significantly surpasses the reference signal and is necessary for the quantification using the ΔΔCt method ($=2^{-(\Delta Ct(\text{group X})-\Delta Ct(\text{control group})}$). The Platinum Taq DNA Polymerase (Invitrogen) and the StepONE Plus cycler (Applied Biosystems, New Jersey, USA) were used.

| | | |
|---|---|---|
| Reaction mixture: | Power SYBR Green PCR Master Mix | 10 µl |
| | Primer forward | 20 pmol |
| | Primer reverse | 20 pmol |
| | cDNA (diluted 1:4) | 2.5 µl |
| | $ddH_2O$ | ad 20 µl |

| PCR stage | Temperature | Time | Cycles |
|---|---|---|---|
| Initial denaturation | 95 °C | 10 min | 1 |
| Denaturation | 95 °C | 15 sec | 40 |
| Annealing | 60 °C | 60 sec | |

### 2.10.5 Isolation of murine DNA for genotyping

DNA of tail tip biopsies of one-month-old mice was isolated using the Phenol/Chloroform-based DNA extraction.

| | | |
|---|---|---|
| Lysis buffer: | Tris | 12.1 g |
| | EDTA | 1.87 g |
| | NaCl | 11.7 g |

Tail tips were incubated in 500 µl lysis buffer supplemented with 2.5 µl Proteinase K (10 mg/ml) at 55 °C and 950 rpm over night in a Thermomixer compact (Eppendorf, Hamburg, Germany). The next day, 500 µl Phenol/Chloroform/Isoamyl alcohol mixture (Carl Roth) were added, samples centrifuged at 14.000 rpm for 10 min (Centrifuge 5424, Eppendorf) at room temperature (RT) and the upper phase transferred to a new tube. After addition of 500 µl

Isopropanol samples were centrifuged at 14.000 rpm and 4 °C for 10 min (Centrifuge 5417 R, Eppendorf), the supernatant discarded, 500 µl of 70% v/v Ethanol added and centrifuged again at 14.000 rpm and 4 °C for 5 min (Centrifuge 5417 R, Eppendorf). Supernatants were discarded, DNA pellets dried for 5 min in the Thermomixer compact (Eppendorf) at 37 °C and dissolved in 50 µl $ddH_2O$.

### 2.10.6 Agarose gel electrophoresis

| | | |
|---|---|---|
| 5x DNA loading buffer: | Xylen cyanol | 25 mg |
| | 0.5 M EDTA | 1.4 ml |
| | Glycerol | 3.6 ml |
| | $ddH_2O$ | 7.0 ml |
| 50x TAE buffer: | Tris | 242 g |
| | Glacial Acetic Acid | 57.1 ml |
| | 0.5 M EDTA | 100 ml |
| | $ddH_2O$ | ad 1 l |

For a 1% w/v agarose gel 1 g agarose was dissolved in 100 ml 1x TAE buffer by heating in a microwave oven. After cooling 6.5 µl ethidium bromide (stock solution 1 mg/ml) per 100 ml gel volume was added and the gel cast. The polymerized gel was transferred to an electrophoresis chamber (Peqlab) filled with 1x TAE buffer and samples diluted in DNA loading buffer loaded. The gels were run at 100 to 140 V. For the estimation of DNA fragment size DNA standards (1 kb or 100 bp standard; NEB) were separated together with the samples. dsDNA with intercalating ethidium bromide was visualized using UV light (312 nm) and the gel documentation system DeVision DBOX (Decon Science Tec, Hohengarden, Germany). For the separation of genotyping PCR fragments 2% w/v agarose gels were used.

### 2.10.7 DNA gel extraction

For the extraction of DNA from agarose gels the corresponding DNA band was cut out of the gel and DNA extracted using the “QIAQuick Gel Extraction Kit” (Qiagen) as defined by the manufacturer. The DNA was eluted using 20 µl $ddH_2O$ and purity and concentration measured by nanodrop spectrophotometer ND 1000 (Peqlab).

### 2.10.8 Restriction of vector DNA and PCR products

The restriction of vector DNA and PCR products for clonation was carried out with 1-3 Units of the corresponding restriction enzymes per µg DNA in the buffer recommended by the manufacturer for 2 hours at 37 °C. Following restriction DNA was separated by agarose gel electrophoresis, vector DNA was de-phosphorylated before separation.

### 2.10.9 De-phosphorylation of DNA

To prevent re-ligation of linearized vector DNA, the 5´-phosphate was removed by treatment with Antarctica Phosphatase (NEB).

| | | |
|---|---|---|
| Reaction mixture: | vector DNA | 2 µg |
| | 10x Antarctica Phosphatase buffer | 5 µl |
| | Antarctica Phosphatase | 1 µl (5 U) |
| | $ddH_2O$ | ad 50 µl |

The reaction mixture was incubated for 30 min at 37 °C and enzymes heat inactivated at 65 °C for 5 min.

### 2.10.10 Ligation of DNA fragments

For the ligation of PCR product and vector DNA a 5:1 ratio (insert:vector) was used and the amount of DNA was calculated using following formula:

mass insert (ng/µl) = 5 x [insert length (bp)/vector length (bp)] x mass vector (ng/µl)

| | | |
|---|---|---|
| Reaction mixture: | vector DNA | x µl (1 part) |
| | insert DNA | y µl (5 parts) |
| | 10x T4 ligase buffer | 2 µl |
| | T4 DNA ligase | 1 µl (400 U) |
| | $ddH_2O$ | ad 20 µl |

The ligation mixture was incubated at 16 °C over night.

### 2.10.11 Transformation of electrocompetent DH10B bacteria

| | | |
|---|---|---|
| LB agar: | Bacto-Tryptone | 10 g |
| | Yeast extract | 5 g |
| | NaCl | 5 g |
| | Agar | 15 g |
| | 1 M NaOH | 1 ml |
| | $ddH_2O$ | ad 1 l |
| | → autoclave | |

One aliquot of DH10B cells (50 µl) per transformation was thawed on ice and 2 µl of the ligation reaction or 1 ng of plasmid DNA added to the bacteria, mixed by pipetting up and down and transferred into a electroporation cuvette (GenePulser 0.1 cm cuvette, Bio-Rad, München, Germany). After the electromagnetic puls of 1.8 kV (MicroPulser, Bio-Rad) 450 µl LB-medium (see 2.10.12) without antibiotics were added and the mixture incubated in a 1.5

ml tube for 1 hour at 150 rpm and 37 °C in a Thermomixer classic (Eppendorf). 100 µl of the bacterial suspension was plated on agar plates with the corresponding antibiotic for the plasmid (100 µg/ml Ampicillin or 33 µg/ml Kanamycin) and incubated at 37 °C over night.

### 2.10.12 Bacterial mini cultures and mini plasmid preparation

| | | |
|---|---|---|
| LB medium: | Bacto-Tryptone | 10 g |
| | Yeast extract | 5 g |
| | NaCl | 5 g |
| | 1 M NaOH | 1 ml |
| | $ddH_2O$ | ad 1 l |
| | → autoclave | |

For mini bacterial cultures 4 ml LB medium containing the corresponding antibiotic for the plasmid (100 µg/ml Ampicillin or 33 µg/ml Kanamycin) were inoculated with a single bacterial colony picked with a sterile pipette tip from agar plates and incubated at 170 rpm and 37 °C over night (Thermomixer, Adolf-Kühner AG, Birsfelden, Germany).

| | | |
|---|---|---|
| P1 buffer: | Tris | 6.06 g |
| | EDTA | 3.72 g |
| | $ddH_2O$ | ad 1 l |
| | adjust pH to 8.0 | |
| | → autoclave | |
| | add 100 mg RNAse I after autoclaving | |
| P2 buffer: | NaOH | 8 g |
| | SDS | 10 g |
| | $ddH_2O$ | ad 1 l |
| P3 buffer: | Potassium Acetate | 294.45 g |
| | $ddH_2O$ | ad 1 l |
| | adjust pH to 5.5 | |

For a mini plasmid preparation 1.5 ml of the mini culture were centrifuged at 14.000 rpm for 30 sec (Centrifuge 5424, Eppendorf) and the pellet resuspended in 250 µl resuspention buffer (P1). After addition of 250 µl lysis buffer (P2) the samples were mixed and incubated for 5 min at RT. Lysis is stopped by addition of 300 µl neutralization buffer (P3) and samples were incubated on ice for additional 5 min. After centrifugation at 14.000 rpm and 4 °C for 10 min the supernatant was transferred to a new tube and the DNA precipitated by addition

of 750 µl of Ethanol and incubation for 5 min at RT. DNA was pelleted by centrifugation at 14.000 rpm and 4 °C for 5 min, washed with 750 µl of 70% v/v Ethanol and after additional centrifugation for 1 min (14.000 rpm, 4 °C) the dried pellet was resuspended in 20 µl dd$H_2O$.

### 2.10.13 Bacterial midi cultures and midi plasmid preparation

For the preparation of bigger amounts of plasmid DNA midi preparations were used. Midi cultures were prepared in a sterile conical flask by addition of 50-500 µl of the corresponding mini culture to 100 ml LB medium containing the appropriate antibiotic (100 µg/ml Ampicillin or 33 µg/ml Kanamycin) and incubation at 37 °C and 170 rpm over night (Thermomixer, Adolf-Kühner AG, Birsfelden, Germany). The bacterial suspension was pelleted at 5000 rcf and 4 °C for 10 min (Centrifuge 5810 R, Eppendorf) and the pellet processed with the "GeneElute HP Plasmid Midiprep Kit" (Sigma Aldrich) as defined by the manufacturer. Purity and concentration of the eluted plasmid was measured by nanodrop spectrophotometer ND 1000 (Peqlab).

### 2.10.14 Sequencing of plasmid DNA

Sequencing of plasmid DNA was performed by Eurofins MWG Biotech (Ebersberg, Germany) following their instructions for DNA preparation. Sequencing results were analyzed by MacVector Ver. 11.1.1 (MacVector Inc., Cary, USA).

## 2.11 Cell culture

### 2.11.1 Cultivation of eukaryotic cell lines

All cell lines were maintained at 37 °C and 5% v/v $CO_2$ in high glucose Dulbecco's modified eagle's medium (DMEM, Invitrogen) supplemented with 1% v/v penicillin/streptomycin (10.000 µg/ml) and 10% v/v fetal calf serum (FCS) (both PAN-Biotech, Aidenbach, Germany). Cell lines were grown as monolayer cultures in cell culture dishes (Nunc, Langenselbold, Germany) and splitted every three to four days when the culture reached about 90% confluency. Cells were washed with Dulbecco's Phosphate Buffered Saline (DPBS, Invitrogen) and after addition of Trypsin-EDTA solution (Invitrogen) incubated for 5 min at 37 °C. Trypsinization was stopped by addition of culture medium and cells pelleted by centrifugation at 500 rcf for 2 min (Centrifuge 5810 R, Eppendorf) to remove residual Trypsin. After resuspention in cell culture medium, 20 µl of the cell suspension were mixed with 20 µl Trypan Blue solution, cells counted in Countess Automated Cell Counter (Invitrogen) and the desired amount of cells added to new dishes with cell culture medium.

### 2.11.2 Thawing and freezing of cell aliquots

| | | |
|---|---|---|
| Freezing medium: | FCS | 90% v/v |
| | DMSO | 10% v/v |

For long-term storage cells were detached and pelleted as described in 2.11.1, the pellet of one confluent 10 cm culture plate (Nunc) resuspended in 1 ml freezing medium and transferred to CryoPure tubes (Sarstedt, Nümbrecht, Germany). Tubes were frozen in NALGENE Mr. Frosty Cryo 1 °C Freezing Container (Thermo Scientific, Rockford, USA) at -80 °C over night and transferred to liquid Nitrogen on the next day.

For reconstitution cells were quickly thawed at 37 °C in a water bath, freezing medium mixed with 10 ml cell culture medium and cells pelleted at 500 rcf for 2 min to remove the cytotoxic DMSO (Centrifuge 5810 R, Eppendorf). The pellet was resuspended in cell culture medium and transferred to 10 cm cell culture plate (Nunc).

### 2.11.3 Transient transfection of cells using Lipofectamine 2000

For transient transfection of HEK293, U2-OS and phoenix-AMPHO cells with plasmid DNA and siRNA cells were grown to 70-90% confluency in cell culture medium without antibiotics. First plasmid DNA and Lipofectamine 2000 were separately diluted in OptiMEM medium (Invitrogen) and incubated for 5 min at RT, following incubation both solutions were combined and incubated for additional 20 min before addition to the cell culture plates. After 6-8 hours the medium was replaced with full cell culture medium. Following volumes were used:

| | 6 well | 6 well | 6 cm plate | 10 cm plate |
|---|---|---|---|---|
| plasmid DNA/siRNA | 5-100 pmol siRNA | 0.3-4 µg plasmid DNA | 1-6 µg plasmid DNA | 5-12.5 µg plasmid DNA |
| Lipofectamine 2000 | 2 µl | 4 µl | 6 µl | 10-25 µl |
| OptiMEM (DNA and Lipofectamine separately) | 250 µl each | 250 µl each | 500 µl each | 1 ml each |

MCF7 cells were also grown to 70-90% confluency in 6 well plates, the plasmid DNA (0.3-4 µg) and 6 µl Lipofectamine 2000 diluted in 250 µl OptiMEM medium separately, incubated for 5 min at RT, then the two solutions mixed together and incubated for additional 20 min. After incubation 500 µl DMEM medium without FCS and without antibiotics were added, the culture medium removed form the dishes and the mixture added to the cells. After 5 hours 1

ml DMEM containing 20% v/v FCS (without antibiotics) was added and cells incubated over night. The next morning the transfection mixture was replaced by full cell culture medium.

### 2.11.4 Generation of retroviruses

For the generation of retroviruses phoenix-AMPHO cells grown on a 10 cm culture plate were transfected with the corresponding plasmids as described in 2.11.3 using 12.5 µg DNA and 25 µl Lipofectamine 2000. 48 hours after transfection the supernatant of the cells was transferred to a sterile 15 ml falcon tube (Sarstedt), remaining cells pelleted by centrifugation at 500 rcf for 2 min (Centrifuge 5810 R, Eppendorf) and the virus containing supernatant transferred to a new falcon. After addition of 80 µg/ml polybrene (Sigma Aldrich) and 80 µg/ml chondroitin sulfate C (Carl Roth) tubes were incubated for 3h at 37 °C and 200 rpm in a shaker (Unimax 1010/Unimax 1000 combination, Heidolph, Schwabach, Germany). Finally the virus was pelleted by centrifugation at 18.000 rcf and 4 °C for 30 min (Centrifuge 5810 R, Eppendorf). Virus pellet was dissolved in adequate culture medium for infection or freezed at -80 °C for storage.

### 2.11.5 Retroviral infection of cells

Cells were grown on 6 cm culture plates to 30% confluency and infected by addition of virus dissolved in cell culture medium containing 10 µg/ml polybrene (Sigma Aldrich). 48 hours after infection selection for infected cells by application of 2 µg/ml puromycin (Carl Roth) containing culture medium was started. Cells were maintained as other cell lines but with culture medium containing puromycin.

### 2.11.6 Cristal violet staining for cell density

Cells were seeded at very low density in 24 well dishes and fed every other day. For measuring cell density, the dish was washed two times with PBS and cells fixed by addition of 400 µl of 1% v/v glutaraldehyde for 15 minutes at room temperature. After washing the dish two times with PBS cells were stained with 0.1% w/v crystal violet solution for 30 minutes. Staining solution was removed, excessive staining solution washed off in a water basin and dish air-dried. Finally crystal violet stain was solubilized by addition of 10% v/v acetic acid and the absorbance at 590 nm measured.

## 2.12 Protein biochemistry

### 2.12.1 Lysis of cell lines

| | | |
|---|---|---|
| Lysis buffer: | 1 M Hepes pH 7.4 | 2 ml |
| | Nonidet P-40 | 1 ml |
| | 0.5 M EDTA | 200 µl |

| | | |
|---|---|---|
| | 5 M NaCl | 3 ml |
| | $ddH_2O$ | ad 100 ml |
| 4x LAEMMLI loading buffer: | 1 M Tris/HCl pH 6.8 | 1.5 ml |
| | 1 M dithiothreitol (DTT) | 3 ml |
| | SDS | 0.6 g |
| | Bromophenol blue | 0.03 g |
| | Glycerol | 3.25 ml |
| | $ddH_2O$ | ad 7.5 ml |

For the preparation of whole cell lysates (WCL) cells were treated as indicate for the individual experiments, cell culture plates were put on ice, washed with ice cold DPBS and ice cold lysis buffer supplemented with phosphatase and protease inhibitors (1 mM DTT, 12.5 mM NaF, 1 mM $Na_3VO_4$, 400 µM phenylarsine oxide, 1 mM phenylmethanesulfonyl fluoride, 10 µg/ml Leupeptin and 10 µg/ml Antipain) was added. Cell suspension was collected with a cell scraper (Sarstedt), transferred to a 1.5 ml tube and incubated for 10 min on ice. After incubation samples were centrifuged for 10 min at 20.000 rcf and 4 °C (Centrifuge 5417 R, Eppendorf) and the supernatant transferred to a new tube. The protein concentration was measured by Bradford protein assay (2.12.3) and 5-25 µg protein, mixed with ¼ of 4x LAEMMLI loading buffer, boiled for 5 min at 95 °C in a Thermomixer classic (Eppendorf) and separated by SDS-PAGE (2.12.4). For the analysis of nuclear proteins the pellet was dissolved in 20 µl 2x LAEMMLI loading buffer, boiled for 5 min at 95 °C in a Thermomixer classic (Eppendorf) and 10 µl separated in SDS-PAGE.

### 2.12.2 (Co-)Immunoprecipitation

| | | |
|---|---|---|
| IP-lysis buffer: | 1 M Tris/HCl pH 8.0 | 5 ml |
| | Nonidet P-40 | 500 µl |
| | NaCl | 0.7 g |
| | $ddH_2O$ | ad 100 ml |
| IP-wash buffer: | 1 M Tris/HCl pH 8.0 | 2 ml |
| | Nonidet P-40 | 500 µl |
| | NaCl | 0.58 g |
| | 0.5 M EDTA | 200 µl |
| | $ddH_2O$ | ad 100 ml |

WCL were prepared as described in 2.12.1 but with ice cold IP-lysis buffer supplemented with phosphatase and protease inhibitors (1 mM DTT, 12.5 mM NaF, 1 mM $Na_3VO_4$, 400 µM phenylarsine oxide, 1 mM phenylmethanesulfonyl fluoride, 10 µg/ml Leupeptin and 10 µg/ml

Antipain). Protein concentration measured by Bradford protein assay (2.12.3) and 500-1000 µg protein incubated with 2 µl V5 antibody (total volume was adjusted to 500 µl by addition of IP-lysis buffer) for 2 hours on an orbital shaker (Intelli-mixer, LTF Labortechnik GmbH & Co. KG, Wasserburg, Germany) at 5 rpm and 4 °C. After addition of 50 µl Dynabeads protein G (Invitrogen) samples were incubated again for 2 hours on an orbital shaker at 5 rpm and 4 °C. After incubation supernatant was discard, beads were washed three times with IP-wash buffer and transferred to a new tube to avoid elution of proteins bound to the tube walls. For the elution of precipitated protein 20 µl 2x loading buffer were added, samples boiled for 5 min at 95 °C in a Thermomixer classic (Eppendorf) and proteins separated by SDS-PAGE (2.12.4).

### 2.12.3 Measurement of protein concentration

To measure the protein concentration in whole cell lysates (WCL) the Bradford protein assay was performed. The Bradford protein assay is a colorimetric protein assay based on an absorbance shift of the dye Coomassie Brilliant Blue G-250 in which under acidic conditions the red form of the dye is converted into its bluer form by complex formation with cationic and non-polar side chains of the proteins. The binding of the dye to the protein stabilizes the blue form and can be measured by the absorbance at 595 nm. For calculation of the protein concentration BSA protein standards are measured as reference.

### 2.12.4 SDS-polyacrylamide gel electrophoresis (SDS-PAGE)

| | | |
|---|---|---|
| 10x SDS running buffer: | Tris | 30 g |
| | Glycine | 144 g |
| | SDS | 15 g |
| | $ddH_2O$ | ad 1 l |
| 4x Upper gel buffer: | Tris | 61 g |
| | 10% w/v SDS | 40 ml |
| | $ddH_2O$ | ad 1 l |
| | adjust pH to 6.7 | |
| 4x Lower gel buffer: | Tris | 182 g |
| | 10% w/v SDS | 40 ml |
| | $ddH_2O$ | ad 1 l |
| | adjust pH to 8.8 | |

The Protean 4 Mini gel electrophoresis chambers (Bio-Rad) were used for gel running. Gel chambers were filled with 1x SDS running buffer, samples denatured by boiling for 5 min at 95 °C in 4x LAEMMLI loading buffer prior to loading and separated at 30 mA per gel and

maximal voltage (Electrophoresis Power Supply – EPS 301, GE Healthcare, München, Germany). The Precision Plus Protein All Blue Standards (Bio-Rad) was used as size marker.

Corresponding to the size of the detected proteins 8-14% polyacrylamid gels were used:

| | **Stacking gel** | **Separating gel** | | |
|---|---|---|---|---|
| | | **8%** | **12%** | **14%** |
| 30% v/v Acrylamide/Bis solution (Bio-Rad) | 0.5 ml | 4 ml | 6 ml | 7 ml |
| 4x Upper buffer | 1.25 ml | | | |
| 4x Lower buffer | - | 3.8 ml | 3.8 ml | 3.8 ml |
| $ddH_2O$ | 3.2 ml | 4.7 ml | 3.7 ml | 1.7 ml |
| Glycerin | - | 2.5 ml | 2.5 ml | 2.5 ml |
| Ammonium persulfate (10% w/v) | 48 µl | 72 µl | 72 µl | 72 µl |
| Tetramethylethylenediamine (TEMED) | 6 µl | 12 µl | 12 µl | 12 µl |

### 2.12.5 Western Blot

| | | |
|---|---|---|
| Transfer buffer: | 1 M Tris/HCl pH 8.3 | 25 ml |
| | Glycine | 11.26 g |
| | Methanol | 100 ml |
| | $ddH_2O$ | ad 1 l |

In SDS-PAGE separated proteins are transferred in an electrical field to PVDF membranes (Millipore) for the immunodetection. Here for a sandwich containing of 3M Whatman paper soaked in transfer buffer, methanol equilibrated PVDF membrane, SDS-gel and again transfer buffer soaked 3M Whatman paper is set up. The transfer was carried out using the Mini Trans-Blot Cell (Bio-Rad) at maximum voltage and 375 mA (Electrophoresis Power Supply – EPS 301, GE Healthcare) for 2 hours.

### 2.12.6 Immunodetection

| | | |
|---|---|---|
| 10x PBS: | NaCl | 80 g |
| | KCl | 2 g |
| | $Na_2HPO_4$ | 14.4 g |
| | $KH_2PO_4$ | 2.4 g |

| | | |
|---|---|---|
| | $ddH_2O$ | ad 1 l |
| | adjust pH to 7.4 | |
| PBS-T: | 10x PBS | 100 ml |
| | Tween 20 | 500 µl |
| | $ddH_2O$ | ad 1 l |
| Blocking solution: | milk powder | 1 g |
| | PBS-T | ad 25 ml |
| Antibody buffer: | BSA | 0.5 g |
| | $NaN_3$ (0.02% w/v stock solution) | 100 µl |
| | PBS-T | ad 10 ml |
| Stripping buffer: | Glycine | 15 g |
| | SDS | 1 g |
| | $ddH_2O$ | ad 1 l |
| | adjust pH to 2.0 | |

To block unspecific binding of antibodies the membrane was incubated on a tumbling table at 25 rpm and RT (WT12, Biometra, Göttingen, Germany) for 2h in blocking solution. Before addition of the primary antibodies the membrane was washed with PBS-T. Primary antibodies were diluted in antibody buffer as indicated in 2.2 and incubated at 25 rpm and 4 °C over night. After incubation with primary antibody the membranes were washed six times for 5 min in PBS-T, the corresponding secondary antibody diluted in PBS-T incubated for 2h at RT and membrane washed again six times for 5 min in PBS-T. The horseradish peroxidase (HRP) coupled to the secondary antibodies was used to detect the proteins by chemiluminescence using the ECL Plus Kit (GE Healthcare, München) and the chemiluminescence reader LASmini4000 (FUJIFILM, Düsseldorf, Germany).

For detection of a second protein on the same PVDF membrane the membrane was stripped by two times 20 min incubation with stripping buffer at 50 °C, washed with PBS-T and detected with the next antibody starting from the blocking step of the membrane.

### 2.12.7 $^{35}$S pulse-chase

To follow a specific protein population over time $^{35}$S pulse-chase assays were performed. HEK293 cells were transfected (2.11.3) with V5-IRS1, myc-Fbw8, LT-antigen or Δ69-83 LT-antigen plasmids, respectively. 24 hours posttransfection cells were washed two times with warm PBS and incubated with depletion medium (methionine and cysteine free DMEM medium, PAN Biotech) supplemented with 10 mM HEPES pH 7.4, 1% v/v L-glutamine and

1% v/v penicillin/streptomycin (both PAN Biotech) for 45 min at 37 °C and 5% v/v $CO_2$. New synthesized proteins were labeled exchanging depletion medium with labeling medium (depletion medium containing 50 µCi/ml $^{35}S$ labeled methionine and cysteine, Hartmann Analytic, Braunschweig, Germany) and incubated for 60 min at 37 °C and 5% v/v $CO_2$. After the labeling interval, 2 ml chase medium (DMEM, Invitrogen), supplemented with 10 mM HEPES pH 7.4, 1% v/v penicillin/streptomycin and 10% v/v FCS were added to stop labeling instantly and then exchanged with fresh chase medium. At the end of each chase interval cells were washed twice with ice cold PBS, lysed and lysates subjected to immunoprecipitation (2.12.2). After separation by SDS-PAGE (2.12.4) the gel was incubated for 30 min in enhancer solution (GE Healthcare) and dried at 80 °C. Results were visualized by autoradiography using a Cyclone Plus Phosphor Imager (PerkimElmer, Rodgau, Germany).

### 2.12.8 *In vitro* ubiquitination

The *in vitro* ubiquitination of insect cell-expressed GST-IRS1 1-574 (1.1 pmol) was carried out in the laboratory of our collaboration partner Dr. Zhen-Qiang Pan at the Mount Sinai School of Medicine in New York as described previously in Xu et al. 2012 (86). A reaction mixture (20 µl) containing 50 mM Tris-HCl, pH 7.4, 5 mM $MgCl_2$, 0.5 mM DTT, 2 mM ATP, 2 mM NaF, 10 nM okadaic acid, CRL7 (0.2 pmol), PK-Ub (50 µM), E1 (13 nM), and UbcH5c (1 µM) was incubated at 37°C and increasing amounts of LT protein (0.5-9.0 pmol) added (For isolation of SV40 LT, see (111)). Reaction products were separated by 4-20% SDS-PAGE and analyzed by anti-GST (Santa Cruz) immunoblot analysis.

### 2.12.9 De-phosphorylation of V5-IRS1

For the de-phosphorylation of V5-IRS1 protein the Calf Intestinal Alkaline Phosphatase (CIP, NEB) was used.

| | | |
|---|---|---|
| Reaction mixture: | Protein | 100 µg |
| | 10x NEBuffer 3 | 5 µl |
| | CIP | 5 µl (50 U) |
| | $ddH_2O$ | ad 50 µl |

The reaction mixture was incubated for indicated time intervals at 37 °C and samples afterwards subjected to SDS-PAGE (2.12.4).

## 2.13 Microscopy

### 2.13.1 Immunofluorescence

For immunofluorescence of 8 µm cryo-sections of 90d old CEA424/SV40 T-antigen transgenic mice tissue the slides were fixed for 20 min in ice cold acetone and blocked in 10% v/v goat serum for 1 hour at RT, washed three times with PBS and incubated with the primary antibodies (1:50) at 4 °C over night. After incubation the primary antibody solution was removed and cells washed three times with PBS. The secondary fluorescence coupled antibodies diluted 1:400 in PBS were incubated for 30 min at RT in a humid chamber. Finally cells were washed again three times with PBS and mounted on glass slides with VECTASHIELD Mounting Medium containing 4´,6´-diamino-2-phenylindole (DAPI) (Vector laboratories, Burlingame, CA).

The following setup was used for image acquisition: Software *MetaMorph Basic Imaging Software* Packets (Molecular Devices, Downingtown, USA), Microscope AxioObserver.Z1 (Zeiss, Jena, Germany), Lumen200 fluorescence illumination system (Prior, Cambridge, UK) and Retiga-4000DC CCD camera (QImaging, Surrey, Canada).

### 2.13.2 Immunohistochemistry

For peroxidase/HE-staining of CEA424/SV40 T-antigen transgenic mice tissue 8 µm slides were fixed 10 min in acetone, endogenous peroxidases were inactivated with 10% v/v methanol/3% v/v $H_2O_2$ in PBS for 5 min and blocked with 1% w/v BSA in PBS for 20 min. Following two hours incubation with primary antibody directed against SV40 T-antigen and incubation with secondary HRP coupled antibody for 1 hour, the peroxidase staining was performed using 0.032% w/v 3-amino-9-ethylcarbazole (AEC; Sigma Aldrich) and 0.036% v/v $H_2O_2$ in 0.13 M acetate buffer pH 5.2 for 15 min. Slides were counterstained for 30 sec with hemalum (Carl Roth). Finally slides were washed with water and mounted using Aquatex mounting medium (Merck).

The following setup was used for image acquisition: Software *MetaMorph Basic Imaging Software* Packets (Molecular Devices, Downingtown, USA), Microscope AxioObserver.Z1 (Zeiss, Jena, Germany) and MicroPublisher 5.0 RTV camera (QImaging, Surrey, Canada).

### 2.13.3 Quantification of and staining intensities

To measure the staining intensity in the tissue sections of CEA424/SV40 T antigen transgenic mice images were acquired using the *MetaMorph Basic Imaging Software* Packets (Molecular Devices, Downingtown, USA) and intensities of defined areas were measured using the ImageJ software (U. S. National Institutes of Health, Bethesda, MD).

Staining intensities were normalized to the corresponding DAPI intensity in the measured areas.

## 2.14 Statistics

Data are presented as means ± SEM. To test the statistical difference between means of two (*t-test*) or more groups (ANOVA following Bonnferoni post-test) and to perform linear regression analysis GraphPad PRISM Ver. 5.0b (GraphPad Software, La Jolla, USA) was used. *P* values $< 0.05$ were considered significant.

# 3 Results[1]

## 3.1 SV40 LT-antigen impairs CRL7 function

To assess the impact of LT-antigen on CRL7 E3 ligase function, the effect of LT-antigen on the degradation of the CRL7 substrate IRS1 was investigated using cell-based degradation assays and *in vitro* ubiquitination assays.

### 3.1.1 LT-antigen expression results in posttranslational stabilization of ectopic IRS1 *

In cell-based degradation assay HEK293 cells were transfected for 48 hours with V5-tagged IRS1 (V5-IRS1), myc-tagged substrate adaptor protein Fbw8 (myc-Fbw8) and HA-tagged wild type or mutant (Δ69-83) LT-antigen. Protein levels of the ectopic expressed V5-IRS1 were analyzed by SDS-PAGE and Western Blot analysis. Over-expression of V5-IRS1 substrate protein resulted in a robust signal compared to empty vector (EV) transfected control cells (Fig. 6, lane 1 vs. 2). As expected, co-expression of the substrate adaptor myc-Fbw8 resulted in a significant 50% decrease in V5-IRS1 protein levels (Fig. 6, lane 3). The reduction in V5-IRS1 protein levels was abolished by administration of the proteasome inhibitor MG132 for 8 hours, indicating the proteasomal kind of the IRS1 degradation (Fig. 6, lane 4).

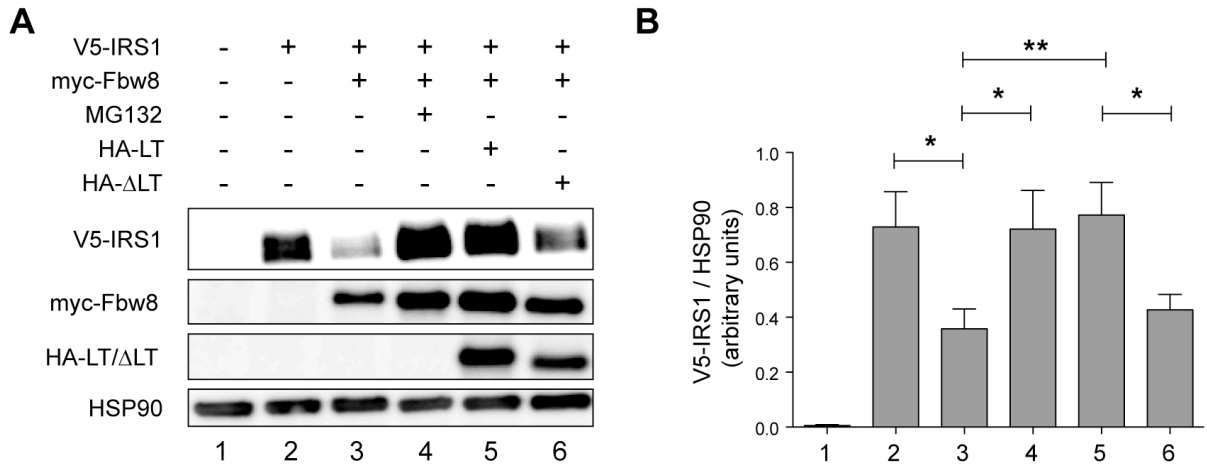


**Fig. 6. Ectopic expressed LT-antigen impairs V5-IRS1 degradation *. A** HEK293 cells were transfected with empty vector (EV) or plasmids encoding V5-tagged IRS1, myc-tagged Fbw8, HA-tagged LT-antigen (LT) and HA-tagged Δ69-83 LT-antigen (ΔLT). MG132 (10 μM) treatment was 8 hours. Lysates were subjected to SDS-PAGE and immunoblot analysis, HSP90 was used as loading control. **B** Quantification of **A**, n=9; * $p < 0.05$; ** $p < 0.01$.

Strikingly, additional co-expression of LT-antigen stabilized V5-IRS1 protein levels to the same extend as proteasomal inhibition by MG132 (Fig. 6, lane 5). In contrast, co-expression

[1] Parts of the results were already published in PNAS (112), corresponding sections and figures are marked with an asterisk (*).

of the CUL7 binding deficient mutant Δ69-83 LT-antigen had no effect on V5-IRS1 degradation (Fig. 6, lane 6). The same results were obtained upon additional expression of flag-tagged CUL7 (flag-CUL7) (Fig. 7). These results suggest a CUL7 dependent effect of LT-antigen on the degradation of IRS1.

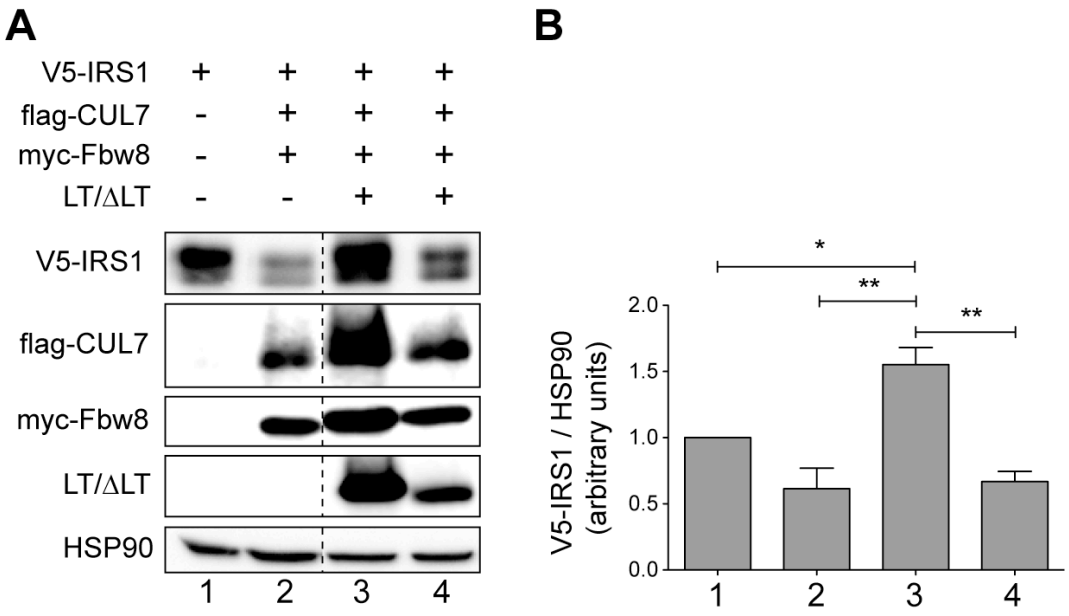


**Fig. 7: Ectopic expressed LT-antigen impairs V5-IRS1 degradation *. A** HEK293 cells were transfected with empty vector (EV) or plasmids encoding V5-tagged IRS1, myc-tagged Fbw8, flag-tagged CUL7, HA-tagged LT-antigen (LT) and HA-tagged Δ69-83 LT-antigen (ΔLT). Lysates were subjected to SDS-PAGE and immunoblot analysis, HSP90 was used as loading control. **B** Quantification of **A**, n=3; * $p < 0.05$; ** $p < 0.01$.

To exclude the possibility that the observed increase in V5-IRS1 protein levels upon LT-antigen expression were due to transcriptional up-regulation, the V5-IRS1 mRNA was measured by quantitative real-time PCR.

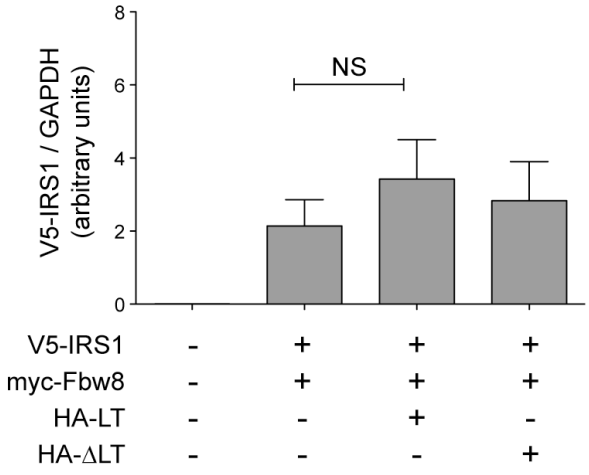


**Fig. 8. LT-antigen over-expression does not change V5-IRS1 mRNA levels *.** HEK293 cells were transfected with plasmids encoding V5-tagged IRS1, myc-tagged Fbw8, HA-tagged LT-antigen (LT) and HA-tagged Δ69-83 LT-antigen (ΔLT). Total mRNA was isolated, cDNA obtained by reverse transcription using polyT primer and analyzed for V5-IRS1 mRNA levels by quantitative real-time PCR. n=5; NS, not significant.

HEK293 cells were transfected with V5-IRS, myc-Fbw8 and LT-antigen or Δ69-83 LT-antigen. Total mRNA was extracted 48 hours after transfection. No significant changes in V5-IRS1 mRNA levels were detected upon co-expression of LT-antigen or Δ69-83 LT-antigen compared to the control group expressing V5-IRS1 and myc-Fbw8 alone (Fig. 8).

To further validate the posttranslational nature of these observations, $^{35}S$ pulse-chase assays were performed to measure V5-IRS1 protein half-life. HEK293 cells were transfected with V5-IRS1 and myc-Fbw8 alone or additionally with LT-antigen or Δ69-83 LT-antigen. 24 hours after transfection, cells were depleted of endogenous methionine and cysteine, followed by radioactive labeling of new synthesized proteins by application of labeling medium containing $^{35}S$ containing amino acids for 1 hour. After labeling, cells were maintained in normal growth medium for 2, 4 and 6 hours (Fig. 9). Cell lysates were subjected to immunoprecipitation with V5 antibody, precipitates separated by SDS-PAGE and dried gels detected by autoradiography. In keeping with previous observations (79), the half-life of V5-IRS1 under co-expression of myc-Fbw8 was 4 hours (Fig. 9, white boxes).

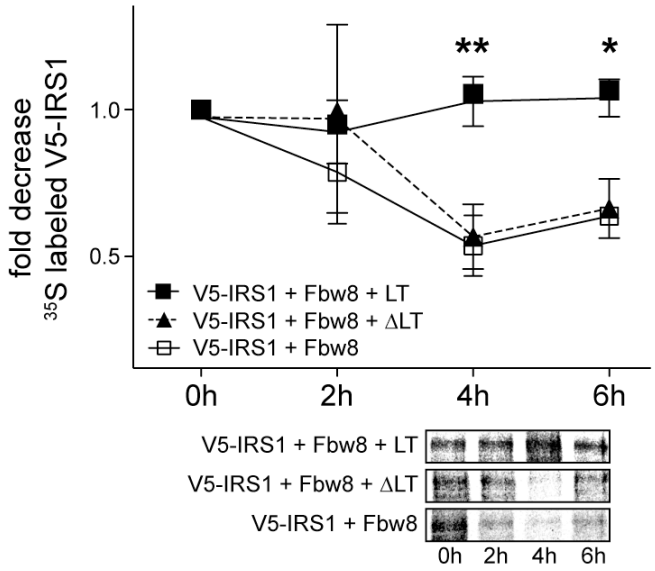


**Fig. 9. LT-antigen expression results in stabilization of V5-IRS1 protein *.** HEK293 cells were transfected with plasmids encoding V5-tagged IRS1, myc-tagged Fbw8, HA-tagged LT-antigen (LT) and HA-tagged Δ69-83 LT-antigen (ΔLT). Following depletion of endogenous methionine and cysteine, new synthesized proteins were labeled by addition of labeling medium containing $^{35}S$ methionine and cysteine. The labeled protein population was chased for 2, 4 or 6 hours. Cell extracts were subjected to V5 immunoprecipitation, separated by SDS-PAGE and visualized by autoradiographic detection of the gels. n=4 (6 hour time point n=3); * $p < 0.05$; ** $p < 0.01$.

The half-life of IRS1 remained unchanged under additional expression of the CUL7 binding deficient mutant Δ69-83 LT-antigen (Fig. 9, black triangles/doted line). In contrast, additional expression of wild type LT-antigen significantly stabilized the V5-IRS1 protein population and resulted in a nearly constant steady state level of V5-IRS1 (Fig. 9, black boxes). Overall,

these observations indicate that LT-antigen by binding to CUL7 results in posttranslational stabilization of the IRS1 substrate protein.

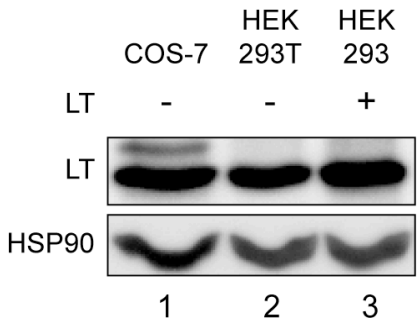


**Fig. 10: Transient expression level of LT-antigen is comparable to LT-antigen level of transformed HEK293T and COS-7 cells *.** Whole cell lysates of COS-7 and HEK293T cells were subjected to SDS-PAGE and immunoblot analysis together with whole cell lysate of LT-antigen (LT) transfected (48 hours) HEK293 cells.

Of note, expression levels of ectopic LT-antigen in these experiments were comparable to the LT-antigen levels found in transformed HEK293T and COS-7 cells (Fig. 10).

### 3.1.2 Degradation of endogenous IRS1

To reproduce these observations in the endogenous system MCF7, U2-OS and HEK293 cells were used. In cellular degradation assays protein levels of endogenous IRS1 were assessed upon transient expression of myc-Fbw8 alone or additional co-expression of flag-CUL7.

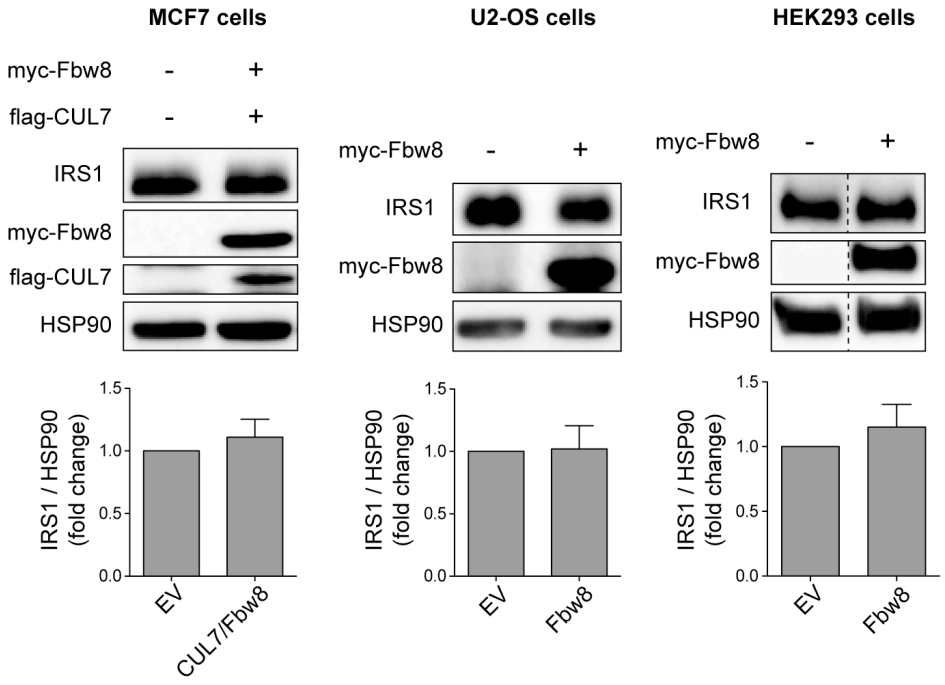


**Fig. 11. No endogenous IRS1 degradation after Fbw8/CUL7 over-expression in different cell lines.** MCF7, HEK293 or U2-OS cells were transfected with myc-tagged Fbw8 alone or with additional co-expression of flag-tagged CUL7 for 48 hours. Lysates were subjected to immunoblot analysis, HSP90 was used as loading control. Quantification n=3 (U2-OS and HEK); n=5 (MCF7).

In contrast to the observed degradation of ectopic expressed V5-IRS1 in HEK293 cells, the endogenous IRS1 protein level in HEK293 cells remained unchanged upon myc-Fbw8 expression. The same results were obtained for over-expression of myc-Fbw8 in U2-OS cells and for over-expression of myc-Fbw8 and additional co-expression of flag-CUL7 in MCF7 cells (Fig. 11). Immunoblot analysis for differences between ectopic expressed V5-IRS1 and endogenous IRS1 revealed increased expression levels of ectopic V5-IRS1 compared to endogenous IRS1 protein levels (Fig. 12A). In addition V5-IRS1 was migrating in two bands compared to one fast migrating band observed for the endogenous protein (Fig. 12A).

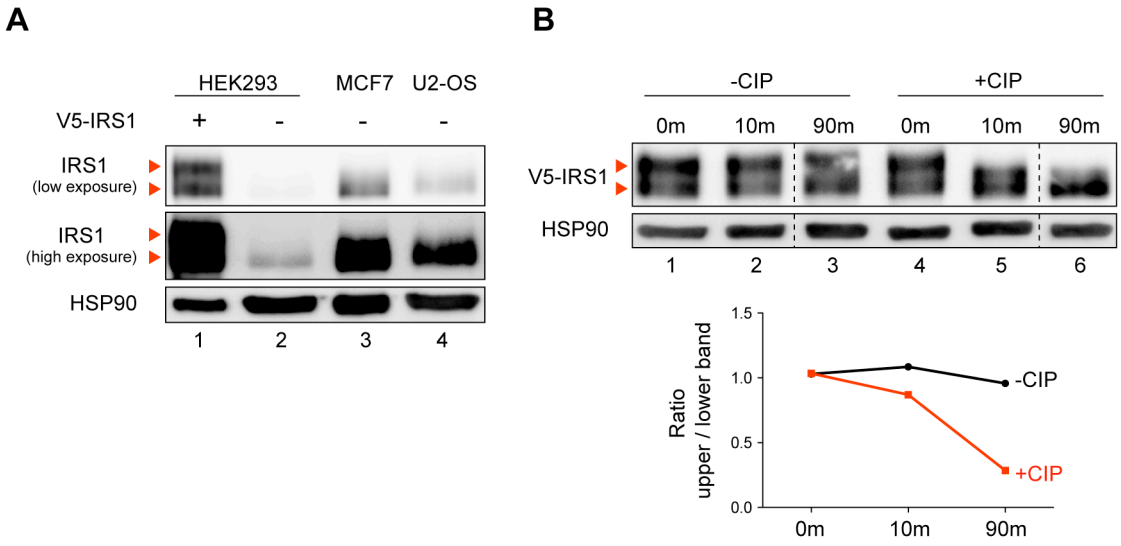


**Fig. 12. Ectopic expressed V5-IRS1 is hyper-phosphorylated. A** Whole cell extract of HEK293 cells transfected with V5-IRS1 and lysates of untransfected HEK293, MCF7 and U2-OS cells were compared for the total IRS1 levels by immunoblot analysis, HSP90 was used as loading control. High and low exposure of the IRS1 detection are shown. **B** Whole cell extract of HEK293 cells transfected with V5-IRS1 were subjected to calf intestinal phosphatase treatment (+CIP) or as control incubated with the reaction mixture without the enzyme (-CIP). The graph displays the ratio upper vs. lower band of the V5-IRS1 detection. Experiment was repeated 3 times, representative results shown.

To test if the additional slower migrating band found for ectopic expressed V5-IRS1 corresponds to a high-phosphorylated IRS1 protein population, lysates of V5-IRS1 transfected HEK293 cells were treated with calf intestinal phosphatase (CIP) for 10 or 90 minutes and samples were subjected to immunoblot analysis. While the control group displayed a constant ratio of upper vs. lower band, CIP treatment resulted in a 75% reduction in the ratio upper vs. lower band after 90 minutes (Fig. 12B).

This argues for two differently phosphorylated V5-IRS1 protein populations, one hypo-phosphorylated and one hyper-phosphorylated, corresponding to the lower or upper band, respectively.

### 3.1.3 LT-antigen impairs IRS1 *in vitro* ubiquitination by CRL7 *

To evaluate if LT-antigen mediated effects on V5-IRS1 degradation were due to direct interference of LT-antigen with the CRL7 ubiquitination function, *in vitro* ubiquitination assays using purified proteins were performed by the laboratory of Pan (New York, USA). Pan and colleagues identified the signal sequence for IRS1 degradation on the N-terminal part (amino acids 1-574) of IRS1 (79, 86). The N-terminal 574 aa of IRS1 were purified as GST-tagged protein (GST-IRS1 1-574) from baculovirus infected High Five insect cells. The ubiquitination was reconstituted by incubation of the GST-IRS1 1-574 with CRL7, UbcH5c (E2 enzyme), E1 enzyme and ubiquitin *in vitro*. CRL7 was isolated from extracts derived from HEK293 cells transfected with flag-CUL7 and myc-Fbw8 plasmids by precipitation with M2-agarose beads. The extend of IRS1 ubiquitination was measured by separation of the reaction products by SDS-PAGE and immunoblot analysis with anti-GST antibody. In the presence of all components formation of high molecular weight protein species, corresponding to ubiquitinated substrate protein, was observed (Fig. 13A, lane 3 vs. 2). The achieved reduction of substrate protein was approximately 70% compared to control conditions without E2 or E3 proteins in the reaction mixture (Fig. 13A, lane 3 vs. 1 and 2).

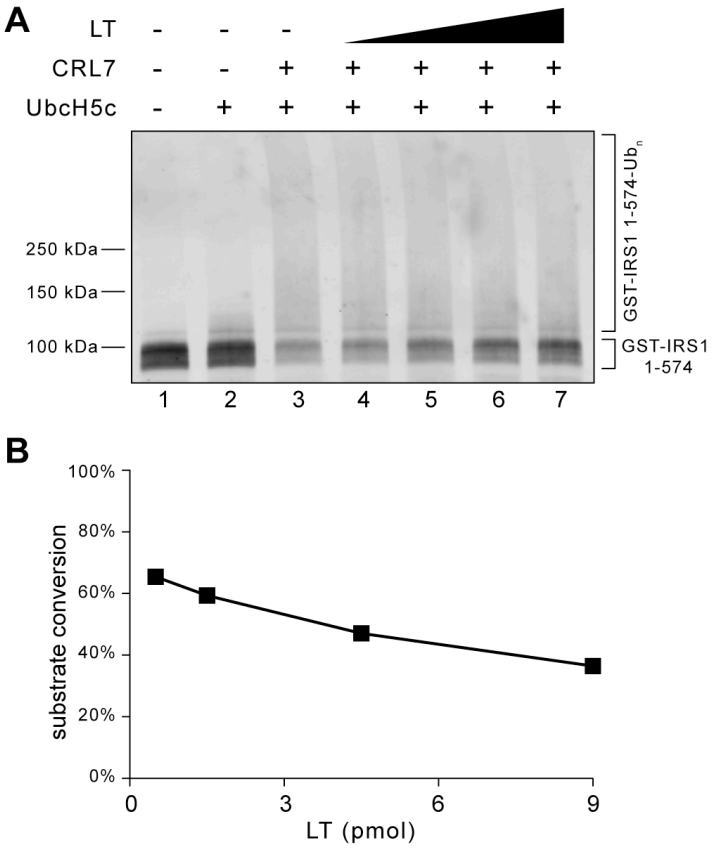


**Fig. 13. Effect of SV40 LT-antigen on the ubiquitination of IRS1 by CRL7 *. A** The *in vitro* ubiquitination reaction was reconstituted as described in (86) and increasing amounts of purified SV40 LT-antigen (LT) (0.5, 1.5, 4.5 and 9 pmol) added. **B** Quantification of input substrate levels after reaction illustrating an inhibitory effect of LT-antigen (courtesy of Prof. Dr. Z.-Q. Pan).

Of note, addition of increasing amounts of purified LT-antigen protein (0.5 – 9 pmol) to the ubiquitination reaction resulted in higher amounts of unmodified IRS1 substrate protein (Fig. 13A, lane 4-7 and Fig. 13B), an indication for reduced substrate ubiquitination.

These results are consistent, with the observed posttranslational stabilization of V5-IRS1 upon LT-antigen expression and indicate IRS1 protein stabilization through impairment of CRL7 ubiquitination function.

## 3.2 The biological relevance of LT-antigen binding to CUL7

To evaluate the biological relevance of SV40 LT-antigen binding to CUL7, the effect of LT-antigen on the signaling pathways downstream of the CRL7 substrate IRS1 were assessed in *in vitro* and *in vivo* experiments. IRS1 is the central mediator in the IGF-1 and insulin signaling pathways. Receptor activation results in recruitment of IRS1 to the receptor, tyrosine phosphorylation of IRS1 and activation of the pro-proliferative and anti-apoptotic downstream pathways PI3K/AKT and Erk MAPK (84). CRL7 was shown to be part of a negative feedback loop involving IRS1 degradation after serine phosphorylation via the mTORC1/S6K1 to restrain IRS1 signaling (79, 86).

### 3.2.1 LT-antigen enhances activation of IRS1 downstream signaling pathways *

To analyze the effect of LT-antigen expression on the activation of the IRS1 downstream pathways, U2-OS cells were transfected with EV, LT-antigen or Δ69-83 LT-antigen encoding plasmids. 48 hours posttransfection, cells lysates were subjected to Western Blot analysis for levels of Ser473 phosphorylated AKT (P-AKT) and Thr202 and Tyr204 phosphorylated Erk1/2 (P-Erk) protein. In keeping with previous results by Alwine et al. LT-antigen expression induced a significant increase in AKT phosphorylation on Ser473 (113).

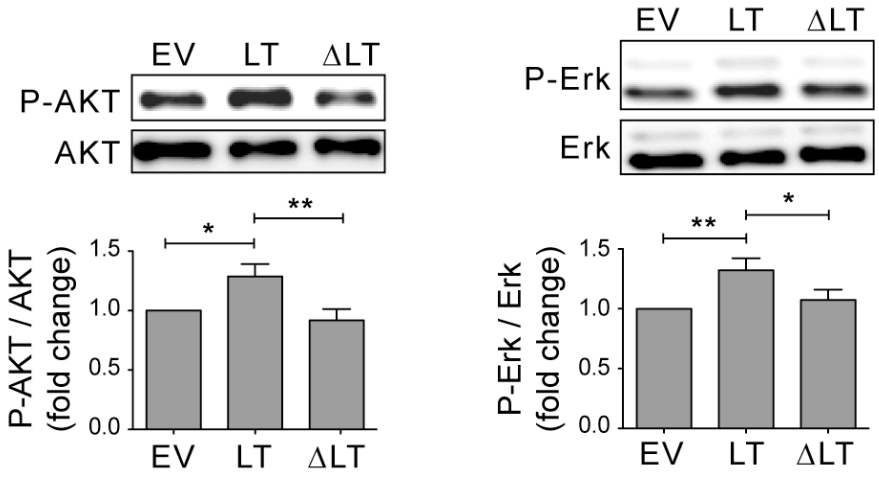


**Fig. 14. Activation of PI3K/AKT and Erk MAPK signaling upon LT-antigen expression in U2-OS cells *.** U2-OS cells were transfected with empty vector plasmid or plasmids encoding HA-tagged LT-antigen (LT) or Δ69-

83 LT-antigen (ΔLT). Lysates were subjected to immunoblot analysis, HSP90 was used as loading control. Quantification n=10; * $p < 0.05$; ** $p < 0.01$.

In addition to the increased AKT activation, a significant 32% up-regulation of the Erk MAPK was observed compared to control conditions (Fig. 14). The same results were obtained upon LT-antigen expression in HEK293 cells (Fig. 15, lane 1 vs. 2). Strikingly, expression of the CUL7 binding deficient Δ69-83 LT-antigen had no effect on the activation levels of both, AKT and Erk MAPK signaling pathways (Fig. 14/Fig. 15, lane 1 vs. 3).

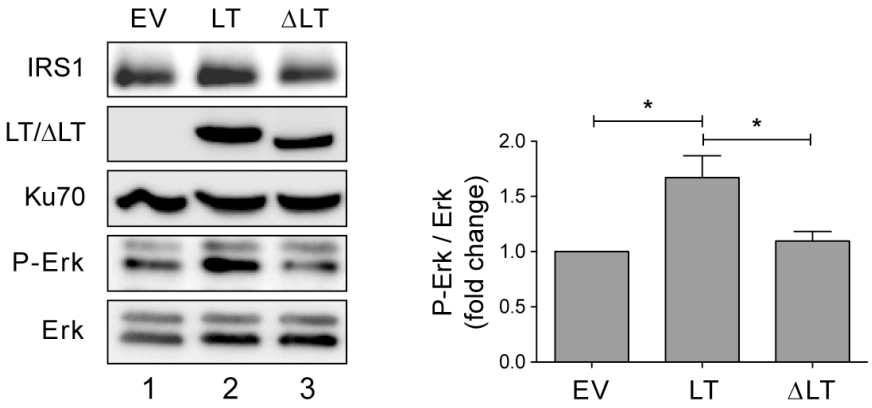


**Fig. 15: Activation of the Erk MAPK signaling pathway upon LT-antigen expression in HEK293 cells *.** HEK293 cells were transfected with empty vector plasmid or plasmids encoding HA-tagged LT-antigen (LT) or Δ69-83 LT-antigen (ΔLT). Lysates were subjected to immunoblot analysis, HSP90 was used as loading control. Quantification n = 4; *P < 0.05.

The observed inhibitory effect of LT-antigen on CRL7, suggested that depletion of CUL7 should exert similar effects on the IRS1 downstream signaling. To test this, U2-OS cells were transfected with scramble (scr) siRNA and siRNA directed against Cul7 mRNA. 48 hours posttransfection, lysates were analyzed by immunoblot analysis.

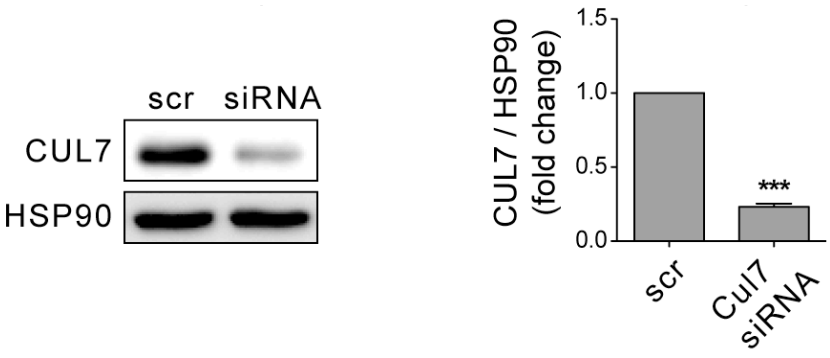


**Fig. 16: CUL7 siRNA depletion *.** U2-OS cells were transfected with scramble control (scr) siRNA or siRNA directed against Cul7 mRNA. Lysates were subjected to immunoblot analysis, HSP90 was used as loading control. Quantification n=4; *** $p < 0.001$.

The achieved CUL7 knockdown efficiency was approximately 80% (Fig. 16). CUL7 depletion significantly enhanced the phosphorylation of AKT at Ser473 by 1.7-fold (Fig. 17, left panel) and of Thr202 and Tyr204 on Erk by 1.2-fold (Fig. 17, right panel).

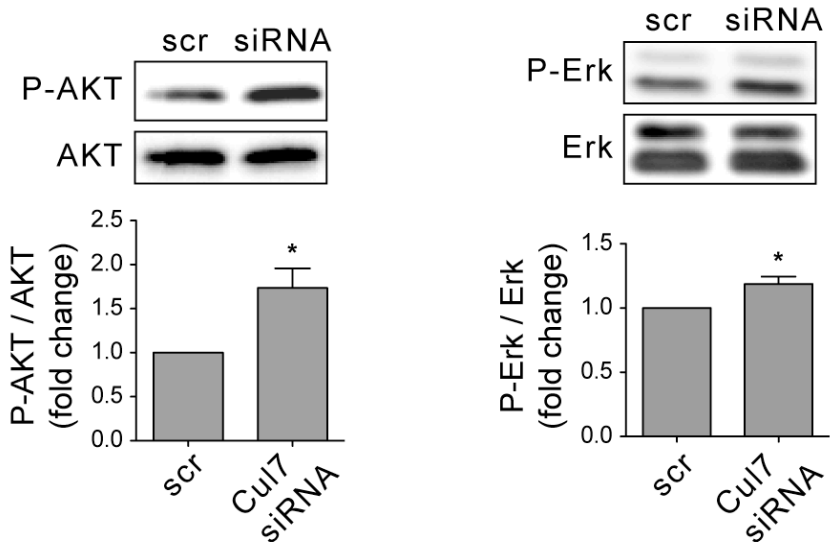


**Fig. 17: Activation of PI3K/AKT and Erk MAPK signaling upon CUL7 siRNA depletion in U2-OS cells *.** U2-OS cells were transfected with scramble control (scr) siRNA or siRNA directed against Cul7 mRNA. Lysates were subjected to immunoblot analysis. Quantification n=4-5 * $p < 0.05$; *** $p < 0.001$.

To further elucidate the effect of LT-antigen over-expression and CUL7 siRNA knockdown in U2-OS cells, the effect on the Erk downstream target *c-fos* (114) was analyzed by quantitative real-time PCR in the laboratory of Dr. Muehlich (LMU, Munich). U2-OS cells transfected with siRNA directed against CUL7 displayed a 9.3-fold up-regulation of *c-fos* when compared to scramble controls (Fig. 18, left panel).

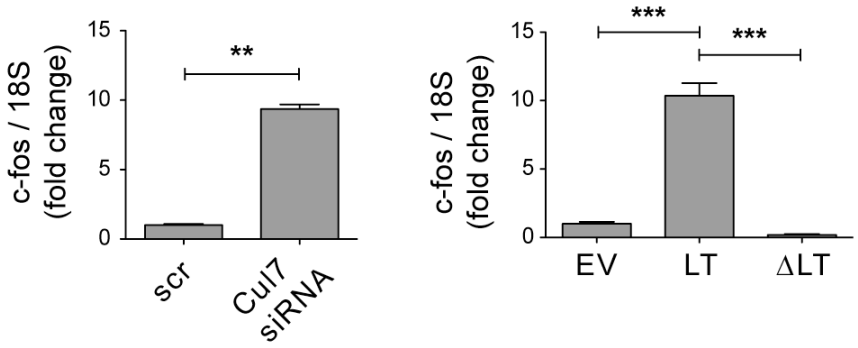


**Fig. 18: *c-fos* mRNA up-regulation upon CUL7 siRNA depletion or LT-antigen expression *.** U2-OS cells were transfected with scramble control (scr) siRNA or siRNA directed against Cul7 mRNA (left panel) or U2-OS cells were transfected with empty vector plasmid or plasmids encoding HA-tagged wild (LT) type or Δ69-83 LT-antigen (ΔLT) (right panel). Total mRNA was isolated, cDNA obtained by reverse transcription using polyT primer and analyzed for *c-fos* mRNA levels by quantitative real-time PCR. n=3; ** $p < 0.01$; *** $p < 0.001$ (courtesy of Dr. Muehlich).

In addition, ectopic expression of LT-antigen resulted in a 10.4-fold up-regulation of *c-fos* when compared to EV transfected control cells (Fig. 18, right panel). Of note, no significant changes of *c-fos* gene expression were observed upon expression of the CUL7 binding-deficient mutant Δ69-83 LT-antigen.

### 3.2.2 Stable LT-antigen expression results in increased proliferation of U2-OS cells *

To examine if the increased activation of the AKT and Erk pathways observed results in increased proliferation, U2-OS cells constitutively expressing EV, LT-antigen or Δ69-83 LT-antigen were generated by retroviral infection. Proliferation was measured by seeding equal numbers of cells in 24 well dishes, cells were fed each other day and growth density was determined by crystal violet staining on the indicated days (Fig. 19B).

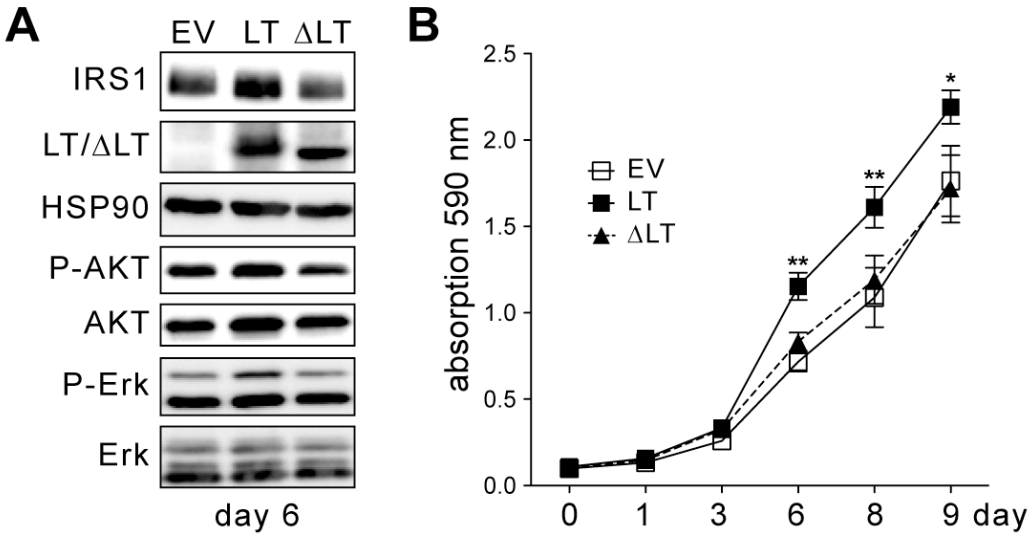


**Fig. 19. Effect of LT-antigen expression on U2-OS cell proliferation rate *.** U2-OS cells were infected with retroviruses containing just the antibiotic resistance (EV control), LT-antigen (LT) or Δ69-83 LT-antigen (ΔLT). **A** Representative immunoblot analysis of lysates of all three stable U2-OS cell lines at day 6 for expression levels of wild type and Δ69-83 LT-antigen, protein level of IRS1 and phosphorylation levels of AKT and Erk. **B** The same amounts of U2-OS cells stably expressing EV control (white boxes), wild type LT-antigen (black boxes) or Δ69-83 LT-antigen (black triangles) was seeded in 24 well dishes and cells fed each other day. At the indicated time points growth density was assessed by crystal violet staining. n=8; * $p < 0.05$; ** $p < 0.01$.

While the EV control infected cells (white boxes) and the Δ69-83 LT-antigen cells (black triangles) displayed the same proliferation rate, the wild type LT-antigen infected cells (black boxes) showed significant higher cell densities from day 6 on. In agreement with the higher proliferation rate, increased levels of IRS1, P-AKT and P-Erk were found in test lysates of cells on day 6 (Fig. 19A).

These data support the hypothesis that binding of SV40 LT-antigen to CUL7 impairs CRL7's function to restrain IRS1 downstream signaling, resulting in increased AKT and Erk MAPK phosphorylation and growth promotion.

### 3.2.3 LT-antigen positive carcinoma display elevated IRS1 protein level and signaling *in vivo* *

To assess the effects of LT-antigen on IRS1 protein homeostasis and downstream signaling *in vivo*, tumor tissue of CEA424/SV40 T-antigen transgenic mice, an established animal model of early-onset invasive gastric carcinoma (110), was examined. These mice express

the LT-antigen protein under the control of a 424 bp region of the gut-specific carcinoembryonic antigen (CEA) and develop multi-focal gastric tumors in 100% of the offspring.

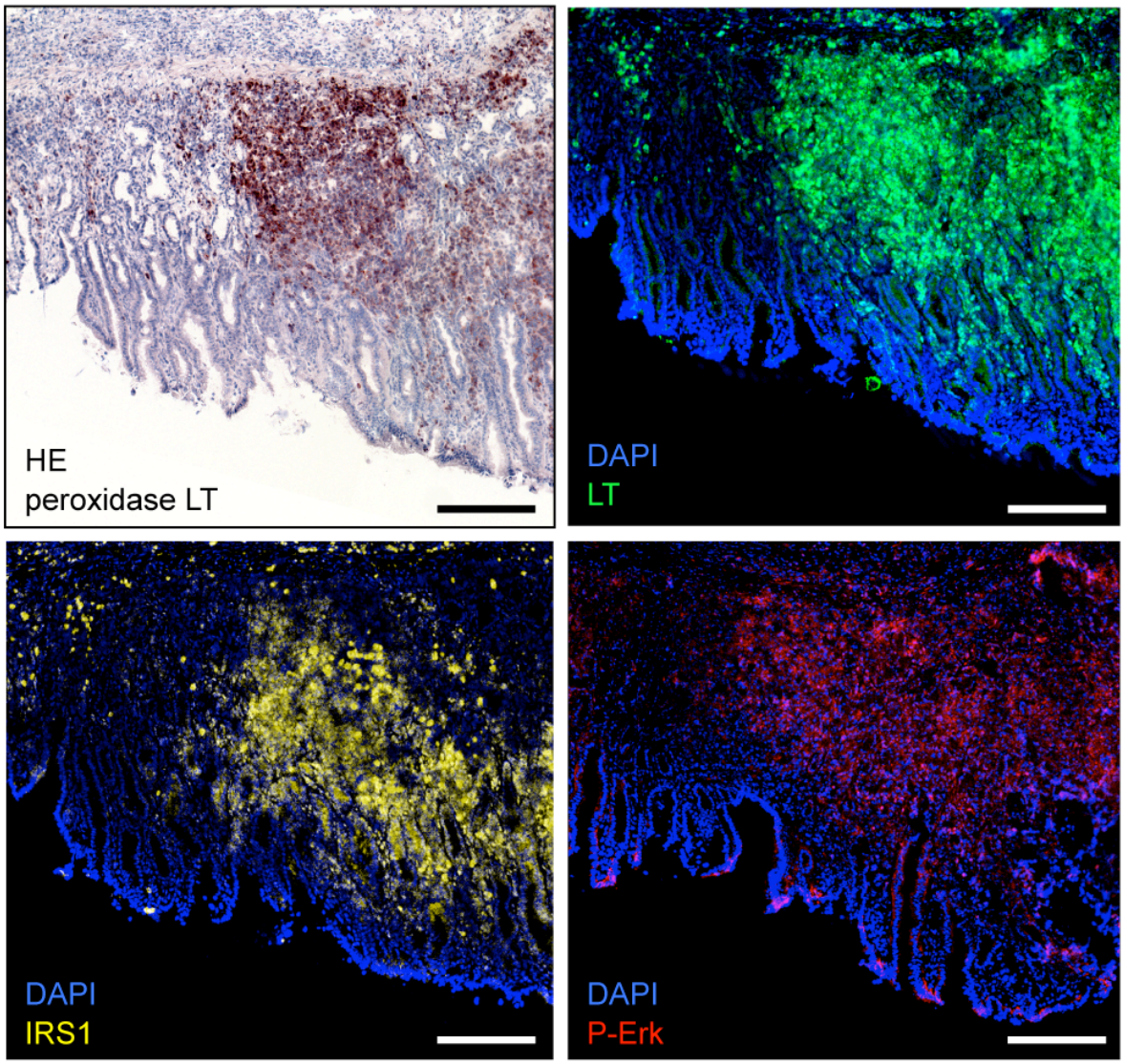


**Fig. 20. Increased IRS1 protein level and Erk MAPK signaling in carcinomas of CEA424/SV40 T-antigen transgenic mice *.** Peroxidase/HE staining (left upper quadrant) or immunofluorescence for LT (green), IRS1 (yellow), P-Erk (red) and nuclear co-staining with DAPI (blue) of pyloric tissue in 90 day-old CEA424/SV40 T-antigen transgenic mice. Scale bar 100 µm.

Tumors develop in the mucosal layer of the pyloric region from day 30 on and mice getting moribund around day 100 to 130, when the tumors penetrate all tissue layers of the stomach (110). Histopathological analysis of gastrointestinal tissue of 90-day-old mice was performed by immunofluorescence microscopy. In keeping with previous reports (115), CEA promoter-driven SV40 LT-antigen expression was associated with substantial malignant transformation of the pyloric and duodenal mucosal layer with formation of neuroendocrine carcinomas (Fig. 20).

To evaluate if the LT-antigen positive areas are correlated with higher IRS1 protein levels and pro-mitogenic signaling, neighboring slides were stained with antibodies directed against LT-antigen (Fig. 20, upper right), IRS1 (Fig. 20, lower left) and Thr202 and Tyr204 phosphorylated Erk1/2 (P-Erk; Fig. 20, lower right). Signal intensities were quantified using the ImageJ software and normalized to DAPI intensities.

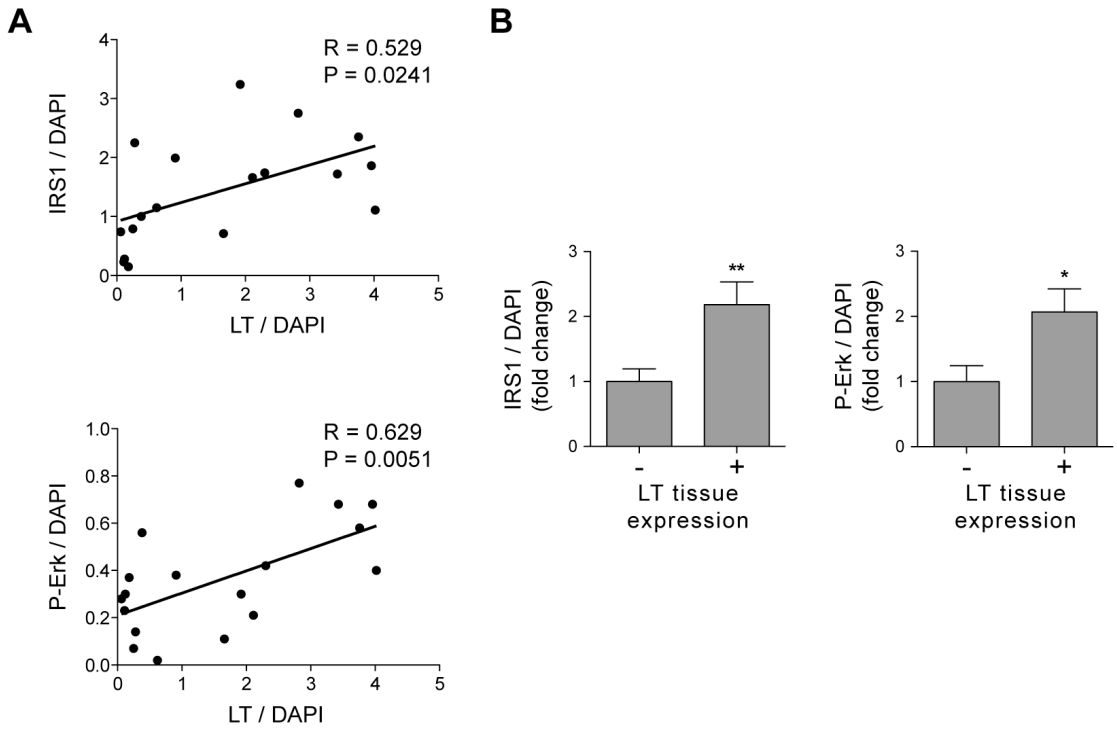


**Fig. 21. Quantification and statistical analysis of IRS1 protein expression and Erk MAPK phosphorylation level in CEA424/SV40 T-antigen transgenic mice *. A** Regression analysis of LT-antigen expression with IRS1 (upper panel) or P-Erk staining intensities (lower panel). **B** Quantification of the mean intensities of IRS1 (left panel) and P-Erk (right panel) in LT positive vs. negative tissue. 18 randomly selected areas of four different tissue samples were quantified using ImageJ software (NIH, Bethesda, MD) and normalized to DAPI intensities. * $p < 0.05$; ** $p < 0.01$.

The expression of LT-antigen in tumorous tissue areas was found positively correlated with both elevated IRS1 protein level (R=0.529, P=0.0241) and activation of the downstream Erk MAPK pathway (R=0.629, P=0.0051; Fig. 21A). When compared to untransformed LT-antigen negative tissue, the mean increase of IRS1 protein and phosphorylated Erk (Thr202 and Tyr204) was approximately 2-fold (Fig. 21B). Interestingly, IRS1 accumulation was not homogenously distributed in the LT-antigen expressing cells, but most prevalent in the SV40 LT-antigen positive cells infiltrating the lamina mucosae (Fig. 20).

Thus, the *in vivo* findings are in accordance with the data obtained from the cell-based and *in vitro* experiments and strongly suggest that SV40 LT-antigen inhibits CRL7 function, which results in deregulated IRS1 signaling.

## 3.3 Molecular mechanism of CRL7 inhibition by LT-antigen *

To gain first insights into the molecular mechanism by which LT-antigen binding to CUL7 interferes with CRL7 E3 ligase function, the LT binding region on CUL7 was mapped. DeCaprio and co-workers already identified the amino acid residues 69-83 on LT-antigen as CUL7 interaction domain and showed that all CRL7 components co-immunoprecipitate with LT-antigen (26).

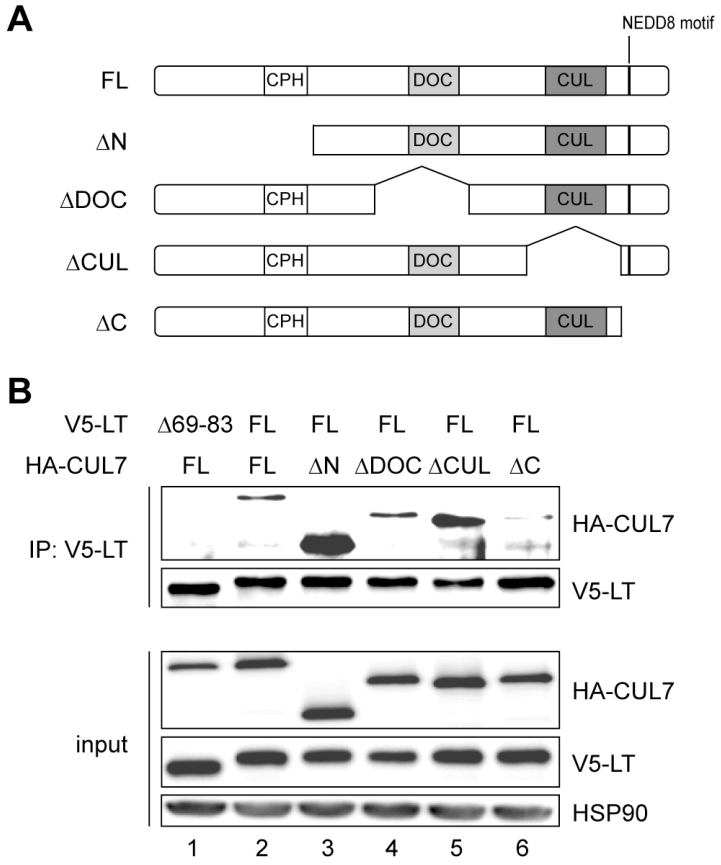


**Fig. 22. LT-antigen binds to the C-terminus of CUL7 *. A** Domain map of full-length (FL) CUL7 and deletion mutants of CUL7 (ΔN, ΔDOC, ΔCUL and ΔC) used for the mapping of CUL7/LT-antigen interaction site on CUL7. CUL7 domains: CPH domain, conserved in CUL7, PARC and HERC2 mediating p53 binding; DOC domain of unknown function; CUL, cullin homology (CH) domain for ROC1 binding; and the extreme C-terminus, harboring the predicted neddylation site (NEDD8 motif). **B** HEK293 cells were transfected with the V5-tagged LT-antigen or Δ69-83 LT-antigen and the indicated HA-tagged CUL7 construct (FL, ΔN, ΔDOC, ΔCUL or ΔC). Cell lysates were subjected to V5 immunoprecipitation and analyzed by immunoblot detection. Whole cell lysates were analyzed for equal expression levels of LT, ΔLT and CUL7 variants by immunoblot analysis, HSP90 was used as loading control. Representative Western blot of four independent experiments.

The CUL7 protein comprises 1698 amino acids and contains several distinct domains: the N-terminal CPH domain, conserved in CUL7, PARC and HERC2 and involved in p53 binding; the DOC domain with a yet unknown function; the cullin homology domain for ROC1 binding; and the C-terminal part including the predicted neddylation site (Fig. 22A). To define the binding region of LT-antigen on CUL7 different HA-tagged truncation mutants of CUL7 lacking either the N-terminal part (ΔN), the DOC domain (ΔDOC), the cullin homology domain (ΔCUL) or the C-terminus (ΔC) (Fig. 22A) were co-expressed with V5-

tagged full-length (FL) LT-antigen in HEK293 cells. Cell lysates were analyzed for CUL7/LT-antigen interaction in co-immunoprecipitation (co-IP) experiments using V5 antibody for the IP. To guarantee equal expression levels of all truncation mutants, crude lysates of all samples were subjected to immunoblot analysis (Fig. 22B, lower part). As negative control for the CUL7/LT-antigen interaction the full-length CUL7 and the CUL7 binding deficient Δ69-83 LT-antigen were co-expressed and lysates analyzed by co-IP (Fig. 22B, lane 1), co-expression of both FL proteins served as positive control (Fig. 22B, lane 2). The ΔN, ΔDOC and ΔCUL truncations of CUL7 were all found to co-precipitate with LT-antigen (Fig. 22B, lane 3-5). In contrast the C-terminal truncation (ΔC) of CUL7 was not found to co-precipitate with the FL LT-antigen (Fig. 22B, lane 6). The ΔC mutation of CUL7 comprises amino acids 1 to 1390, pointing to a critical role for residues 1391 to 1698 of CUL7 in binding LT-antigen.

# 4 Discussion

Simian virus 40 LT-antigen is a powerful viral oncoprotein with the potential to induce tumors in rodents and transform cells in culture (34, 116). Binding and inactivation of the central tumor suppressor p53 and members of the pRB family by LT-antigen was shown to be essential for driving cells into uncontrolled cell proliferation. However, subsequent studies revealed that interactions of LT-antigen with other host proteins are required for the full transformational phenotype induced by LT-antigen (117). For example the interaction of LT-antigen with CUL7, the scaffold subunit of the Cullin-RING E3 ubiquitin ligase 7 (CRL7), was shown to be necessary for transformation by LT-antigen, independent of its binding and inactivation of p53 and pRB. A CUL7 binding deficient mutant of LT-antigen that is still able to bind to both tumor suppressors, is unable to induce cellular transformation (25, 26). In addition Baserga and co-workers showed that the IGF-1 receptor (IGF-1R) and IRS1 are critical determents for the cellular transformation by LT-antigen. Cells lacking the IGF-1R (103, 104), IRS1 or an active IRS1 signaling via PI3K (105) cannot be transformed by LT-antigen.

The identification of CRL7 as E3 ligase for IRS1 and the involved negative feedback loop for IRS1 degradation (79), provided a possible link between CUL7 and the IRS1 signaling axis in LT-antigen transformation. Based on these previous results the aim of this work, was to assess the effect of LT-antigen on the degradation of IRS1 by the CRL7 E3 ligase, to investigate the effect on the IRS1 downstream signaling and to elucidate the underlying molecular mechanism. The proposed model for LT-antigen binding to CUL7, involves impairment of the E3 ligase function of CRL7, thereby resulting in stabilization of IRS1 and increased pro-mitogenic signaling via the downstream pathways PI3K/AKT and Erk MAPK that could contribute to oncogenic transformation by LT-antigen (Fig. 23).

## 4.1 SV40 LT-antigen impairs CRL7 function

In this work, evidence that binding of LT-antigen to CUL7 impairs the ability of CRL7 to mediate ubiquitin-dependent degradation of IRS1 is provided. Expression of SV40 LT-antigen, but not the CUL7 binding deficient mutant Δ69-83 LT-antigen, results in posttranslational accumulation (Fig. 6-8) and prolonged protein half-life (Fig. 9) of transient expressed V5-IRS1. Further it was shown that LT-antigen inhibits CRL7 mediated poly-ubiquitination of GST-IRS1 1-574 *in vitro* (Fig. 13) and a 2-fold increase in IRS1 levels were found in LT-antigen positive tumorous tissue of CEA424/SV40 T-antigen transgenic mice (Fig. 21B). The observed inhibitory effect on CRL7 is in line with the increase in IRS1 protein level found in *cul7*$^{-/-}$ MEFs compared to wild type MEFs (79) and with the observed

stabilization of endogenous IRS1 levels upon CUL7 siRNA knockdown in C2C12 myotubes (118).

It should be noted that efforts to induce the degradation of endogenous IRS1 by sole over-expression of CRL7 components were unsuccessful in different cell lines (Fig. 11). It was shown that IRS1 degradation by CRL7 is dependent on serine phosphorylation by S6K1, generating a phosphdegron motif as result of a negative feedback loop via the mTORC1/S6K1 axis to restrain IRS1 signaling (79, 86). In addition, prolonged IGF-1 or insulin stimulation resulting in degradation of IRS1 were found to be dependent on the PI3K signaling axis (119–121). The fact that no stimulation was needed for degradation of ectopic expressed V5-IRS1 maybe explained by the high phosphorylation level of V5-IRS1 observed upon over-expression (Fig. 12), similar effects were observed by Lee and co-workers for IRS1 over-expression under *in vitro* and *in vivo* conditions (89). Despite this uncertainty, multiple *in vivo* and *in vitro* results, as summarized above, suggest a role for SV40 LT-antigen in protecting IRS1 from CRL7-mediated degradation.

Beside the mTORC1/S6K1 axis, mTORC2-mediated regulation of Fbw8 (85, 87) was involved in IRS1 protein homeostasis. mTORC2 directly phosphorylates Fbw8 at Ser86, which stabilizes Fbw8 and translocates it to the cytosol, finally resulting in IRS1 degradation. In addition, genetic up-regulation of Fbw8 in MEFs of LKB1 knockout mice was shown to induce degradation of endogenous IRS1. The authors were able to prevented IRS1 degradation by siRNA knockdown of Fbw8 (80). Lately also another protein, TBC1D3, was identified to be involved in controlling IRS1 protein stability in humans. TBC1D3 expression delayed ubiquitination and degradation of IRS1 by suppression of IRS1 serine phosphorylation, finally resulting in increased AKT downstream signaling (88). The same group identified TBC1D3 as a CRL7 substrate and showed that the degradation, analog to IRS1 degradation, is dependent on TBC1D3 phosphorylation upon growth factor stimulation (77).

## 4.2 The biological relevance of LT-antigen binding to CUL7

Human cancers often display increased IRS1 expression levels (100–102) and over-expression of IRS1 in animals was shown to cause tumors (89, 122, 123). IRS1 mediates its pro-mitogenic and anti-apoptotic signaling via the downstream pathways PI3K/AKT and Erk MAPK. Dysregulation and mutations of these downstream pathways were also linked to tumorigenesis and cancer (90–99). At a cellular level, IRS1 and its downstream signaling pathways have been directly linked to cellular transformation by SV40 LT-antigen. It has been shown that signaling through the IGF-1 receptor is essential for transformation by

SV40 LT-antigen (103–105). Cells that do not express IRS1 or contain inactive IRS1 species failed to be transformed in culture in the presence of LT-antigen, which could be overcome by expression of a constitutive active p110 subunit of PI3K (105).

Alwine and co-workers reported that expression of SV40 LT-antigen resulted in elevated AKT activation levels that were prevented by application of the PI3K inhibitor LY294002 (124) or shRNA knockdown of IRS1 (113), suggesting that LT-antigen interferes with the signaling cascade upstream of PI3K and implicating IRS1 as critical component mediating the LT-antigen effect on the signaling pathway.

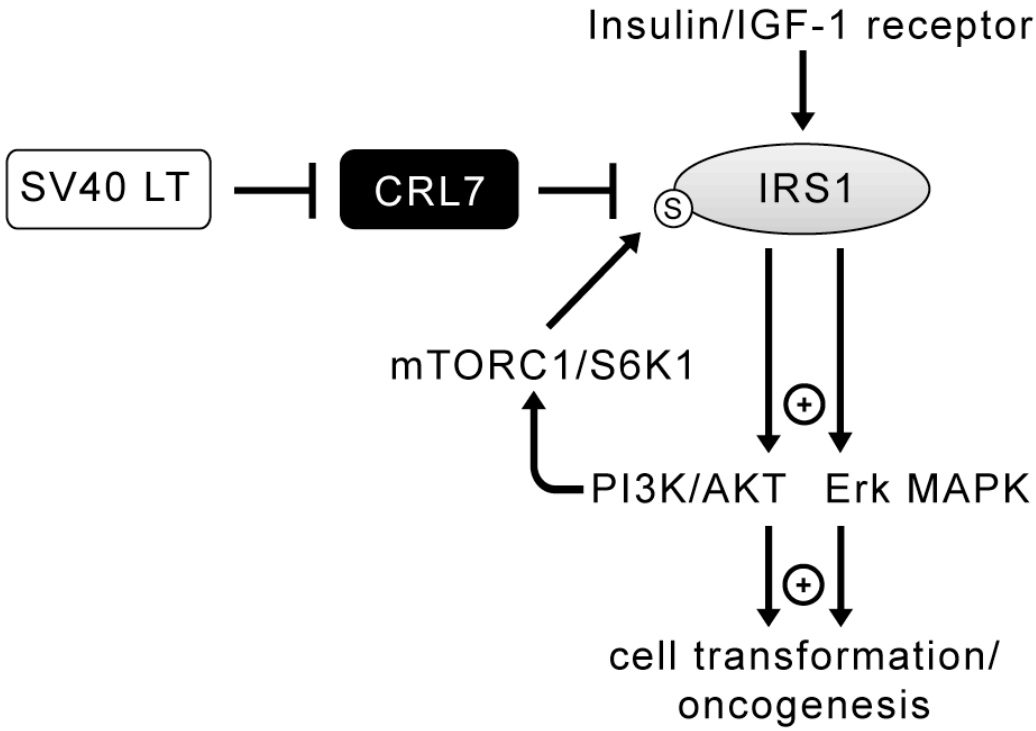


**Fig. 23: A model for the role of LT-antigen interaction with CUL7 *.** CRL7 regulates PI3K/AKT and Erk MAPK signaling pathways via ubiquitin-mediated degradation of IRS1 that is dependent on a negative feedback loop via mTORC1/S6K1. Binding of SV40 LT-antigen (LT) to CUL7 inhibits CRL7 ubiquitin ligase function, resulting in de-suppression and activation of IRS1 downstream signaling pathways. This may contribute to cell transformation and oncogenesis by SV40 (modified from (112)).

In this work, evidence that SV40 LT-antigen expression leads to deregulation of IRS1 downstream signaling pathways AKT and Erk MAPK is provided. Expression of SV40 LT-antigen, but not of CUL7 binding-deficient mutant Δ69-83 LT-antigen (Fig. 14/Fig. 15), or CUL7 depletion (Fig. 17) results in hyper-activation of IRS1 downstream signaling pathways AKT and Erk MAPK and up-regulation of the Erk downstream target gene *c-fos* (Fig. 18). *C-fos* is one of the immediate early genes (IEGs) induced by the nuclear ternary complex factor (TCF), which is directly activated by the Erk MAPK pathway. The IEGs products like c-Fos or c-Myc then induce the late-response genes that promote cell survival, cell division

and cell motility (114). In agreement with the observed hyper-activation of these pathways, U2-OS cells constitutively expressing LT-antigen displayed increased proliferation rates compared to EV and Δ69-83 LT-antigen expressing cells (Fig. 19). In addition, increased activation of the AKT and Erk MAPK pathways were shown in *cul7*$^{-/-}$ MEFs compared to wild type MEFs and in C2C12 myotubes depleted of CUL7 compared to scramble control treated cells (79, 118). Finally, SV40 LT-antigen positive carcinomas of transgenic CEA424/SV40 T-antigen mice exhibited markedly increased IRS1 protein and Thr202 and Tyr204 phosphorylated Erk1/2 levels when compared to non-transformed tissue (Fig. 21).

These findings suggest that SV40 LT-antigen acts to neutralize CRL7 activity, which might contribute to SV40-induced oncogenesis. In this model, SV40 LT-antigen inhibition of CRL7-mediated proteasomal degradation of IRS1 causes sustained pro-mitogenic PI3K/AKT and Erk MAPK signaling that may contribute to cellular transformation (Fig. 23).

A role for a negative feedback loop via IRS1 in controlling cancer was first revealed in a study with mice heterozygous for *Tsc2* (125). TSC2 is an inhibitor of RHEB and hence the loss of TSC2 leads to activation of mTORC1/S6K1. It was shown that *Tsc2* heterozygous mice develop benign haemangiomas due to sporadic loss of the functional *Tsc2* allele. The lack of malignant tumor development results from inactive AKT, because highly activated mTORC1/S6K1 triggers IRS1-mediated negative feedback loop to suppress PI3K. In keeping with this concept, circumventing the IRS1 negative feedback loop by reduction of PTEN activity, resulted in enhanced AKT activation, as well as more frequent and aggressive haemangiomas (125).

Interestingly, the viral early region of SV40 encodes the ST-antigen that supports LT-antigen in cell transformation. It was shown that ST-antigen alone is not sufficient to induce the transformational phenotype of SV40 but can support LT-antigen in the cellular transformation of some cell lines where LT-antigen expression is limited (13). ST-antigen inactivates the serine-threonine protein phosphatase A (PP2A), resulting in increased AKT phosphorylation and signaling (14–16). It is thus tempting to speculate that SV40 LT-antigen and ST-antigen cooperate to activate pro-mitogenic signaling using distinct mechanisms for cellular transformation.

## 4.3 Molecular mechanism of CRL7 inhibition by LT-antigen

DeCaprio and co-workers mapped the CUL7 interaction domain on LT-antigen to the amino acid residues 69-83 and showed that all CRL7 components co-precipitate with the wild type LT-antigen, indicating that LT-antigen does not disrupt the complex formation of CRL7 (26).

In co-immunoprecipitation experiments the C-terminal region of CUL7 was found to be important for LT-antigen binding. The ΔC mutant, comprising amino acids 1 to 1390 of CUL7, did not co-precipitate with full length LT-antigen (Fig. 22), involving amino acid residues 1391 to 1698 as critical residues in the CUL7/LT-antigen interaction.

The C-terminus of most, if not all, cullins is covalently conjugated with the ubiquitin-like molecule NEDD8. Modification with NEDD8, termed neddylation, activates E3 ligase activity of CRLs by promoting substrate poly-ubiquitination (57). In vitro mutagenesis experiments and structural studies have suggested that conjugation of NEDD8 to CUL1 induces conformational changes required for ubiquitin transfer, thereby driving CRLs into an active state (59, 60).

Adjacent to the C-terminus Cullin proteins harbor the conserved Cullin-homology domain (CH) for binding of the RING-finger partner protein ROC1 or ROC2 that recruits the ubiquitin-loaded E2 enzymes for catalysis (48). Based on structural work on the CUL1–ROC1 association (56), CUL7's C-terminus is projected to form multiple interface interactions with the N-terminal S1 ß-strand of ROC1. Interestingly, inhibition of CRL1 E3 ligase function was lately observed by Glomulin binding to ROC1 (73, 74). Glomulin was first found as protein associated with the C-terminus of CUL7 (69), further studies revealed that Glomulin specifically binds to the E2-interacting surface in the RING domain of ROC1 but not ROC2. *In vitro*, Glomulin binding inhibited the ubiquitination activity and also neddylation of CUL1 (73). Further, *in vitro* and *in vivo* loss of Glomulin resulted in increased turnover of the Fbw7 substrate adaptor of the $SCF^{FBW7}$ complex probably due to increased autoubiquitination by the E3 ligase, involving Glomulin in the control of Fbw7 stability (73).

It is tempting to speculate that SV40 LT-antigen inhibition functions similar to E3 ligase inhibition by Glomulin but it remains to be determined whether SV40 LT-antigen impairs CRL7 function through disrupting activities associated with the C-terminus of CUL7 in supporting the ROC1 RING and/or neddylation.

# 5 Summary

SV40 LT-antigen is a well-studied oncoprotein with the potential to induce tumors in rodents and transform mammalian cells in culture. Binding and inactivation of the two central tumor suppressors p53 and pRB is essential for the transformation by LT-antigen. In addition, it was shown that interaction with CUL7 is a prerequisite for LT-antigen transformation. CUL7 is the scaffold protein of the Cullin-RING E3 ubiquitin ligase 7 (CRL7).

This work provides *in vitro* and *in vivo* evidence that SV40 LT-antigen impairs the ubiquitin ligase function of CRL7. The proteasomal degradation of the CRL7 substrate insulin receptor substrate 1 (IRS1), a central component of the insulin and insulin-like growth factor 1 (IGF-1) signaling pathway, is impaired by SV40 LT-antigen but not by its CUL7 binding deficient mutant (Δ69-83 LT-antigen). LT-antigen expression resulted in posttranslational stabilization and prolonged half-life of IRS1. Further it was shown that LT-antigen interacts with the C-terminal region of CUL7, potentially impairing CRL7 function by interference of CUL7 neddylation or E2 binding. *In vitro* the addition of LT-antigen resulted in a clear reduction of ubiquitinated IRS1 substrate protein. The IRS1 downstream signaling pathways PI3K/AKT and Erk MAPK were found up regulated by LT-antigen expression, but not Δ69-83 LT-antigen expression, and CUL7 depletion by RNA interference. Also the Erk MAPK downstream target *c-fos* was found up regulated under both, LT-expression (10.4-fold) and CUL7 depletion (9.3-fold). Cells constitutively expressing LT-antigen displayed increased proliferation compared to control cells expressing EV or Δ69-83 LT-antigen. Finally, SV40 LT-antigen positive carcinoma of CEA424/SV40 T-antigen transgenic mice displayed elevated IRS1 protein levels and increased activation of downstream signaling.

Taken together, these data suggest that SV40 LT-antigen impairs CRL7 function, thereby sustaining high activation levels of pro-mitogenic IRS1 downstream signaling pathways PI3K/AKT and Erk MAPK, which may contribute to SV40 oncogenic transformation.

# 6 References


1. Linzer, DI., Levine, AJ. Characterization of a 54K dalton cellular SV40 tumor antigen present in SV40-transformed cells and uninfected embryonal carcinoma cells. Cell 17 (1979) 43–52

2. DeCaprio, JA., Ludlow, JW., Lynch, D., Furukawa, Y., Griffin, J., Piwnica-Worms, H., Huang, CM., Livingston, DM. The product of the retinoblastoma susceptibility gene has properties of a cell cycle regulatory element. Cell 58 (1989) 1085–95

3. STEWART, SE., EDDY, BE., BORGESE, N. Neoplasms in mice inoculated with a tumor agent carried in tissue culture. J. Natl. Cancer Inst. 20 (1958) 1223–43

4. SWEET, BH., HILLEMAN, MR. The vacuolating virus, S.V. 40. Proc. Soc. Exp. Biol. Med. 105 (1960) 420–7

5. An, P., Sáenz Robles, MT., Pipas, JM. Large T antigens of polyomaviruses: amazing molecular machines. Annu. Rev. Microbiol. 66 (2012) 213–36

6. DeCaprio, J a., Garcea, RL. A cornucopia of human polyomaviruses. Nat. Rev. Microbiol. 11 (2013) 264–76

7. HABEL, K. SPECIFIC COMPLEMENT-FIXING ANTIGENS IN POLYOMA TUMORS AND TRANSFORMED CELLS. Virology 25 (1965) 55–61

8. Poulin, DL., DeCaprio, J a. Is there a role for SV40 in human cancer? J. Clin. Oncol. 24 (2006) 4356–65

9. Thimmappaya, B., Reddy, VB., Dhar, R., Celma, M., Subramanian, KN., Zain, BS., Pan, J., Weissman, SM. The structure of genes, intergenic sequences, and mRNA from SV40 virus. Cold Spring Harb. Symp. Quant. Biol. 42 Pt 1 (1978) 449–56

10. Reddy, VB., Thimmappaya, B., Dhar, R., Subramanian, KN., Zain, BS., Pan, J., Ghosh, PK., Celma, ML., Weissman, SM. The genome of simian virus 40. Science 200 (1978) 494–502

11. Zhu, JY., Abate, M., Rice, PW., Cole, CN. The ability of simian virus 40 large T antigen to immortalize primary mouse embryo fibroblasts cosegregates with its ability to bind to p53. J. Virol. 65 (1991) 6872–80

12. Zhu, J., Rice, PW., Gorsch, L., Abate, M., Cole, CN. Transformation of a continuous rat embryo fibroblast cell line requires three separate domains of simian virus 40 large T antigen. J. Virol. 66 (1992) 2780–91

13. Bikel, I., Montano, X., Agha, ME., Brown, M., McCormack, M., Boltax, J., Livingston, DM. SV40 small t antigen enhances the transformation activity of limiting concentrations of SV40 large T antigen. Cell 48 (1987) 321–30

14. Yuan, H., Veldman, T., Rundell, K., Schlegel, R. Simian virus 40 small tumor antigen activates AKT and telomerase and induces anchorage-independent growth of human epithelial cells. J. Virol. 76 (2002) 10685–91

15. Pallas, DC., Shahrik, LK., Martin, BL., Jaspers, S., Miller, TB., Brautigan, DL., Roberts, TM. Polyoma small and middle T antigens and SV40 small t antigen form stable complexes with protein phosphatase 2A. Cell 60 (1990) 167–76

16. Rodriguez-Viciana, P., Collins, C., Fried, M. Polyoma and SV40 proteins differentially regulate PP2A to activate distinct cellular signaling pathways involved in growth control. Proc. Natl. Acad. Sci. U. S. A. 103 (2006) 19290–5

17. Srinivasan, a., McClellan, a J., Vartikar, J., Marks, I., Cantalupo, P., Li, Y., Whyte, P., Rundell, K., Brodsky, JL., Pipas, JM. The amino-terminal transforming region of simian virus 40 large T and small t antigens functions as a J domain. Mol. Cell. Biol. 17 (1997) 4761–73

18. Campbell, KS., Mullane, KP., Aksoy, I a., Stubdal, H., Zalvide, J., Pipas, JM., Silver, PA., Roberts, TM., Schaffhausen, BS., DeCaprio, J a. DnaJ/hsp40 chaperone domain of SV40 large T antigen promotes efficient viral DNA replication. Genes Dev. 11 (1997) 1098–1110

19. Stubdal, H., Zalvide, J., Campbell, KS., Schweitzer, C., Roberts, TM., Caprio, JADE., DeCaprio, J a. Inactivation of pRB-Related Proteins p130 and p107 Mediated by the J Domain of Simian Virus 40 Large T Antigen. Microbiology 17 (1997) 4979–4990

20. Zalvide, J., Stubdal, H., DeCaprio, J a. The J domain of simian virus 40 large T antigen is required to functionally inactivate RB family proteins. Mol. Cell. Biol. 18 (1998) 1408–15

21. Sullivan, CS., Gilbert, SP., Pipas, JM. ATP-dependent simian virus 40 T-antigen-Hsc70 complex formation. J. Virol. 75 (2001) 1601–10

22. Waga, S., Bauer, G., Stillman, B. Reconstitution of complete SV40 DNA replication with purified replication factors. J. Biol. Chem. 269 (1994) 10923–34

23. Wu, X., Avni, D., Chiba, T., Yan, F., Zhao, Q., Lin, Y., Heng, H., Livingston, D. SV40 T antigen interacts with Nbs1 to disrupt DNA replication control. Genes Dev. 18 (2004) 1305–16

24. Zhao, X., Madden-Fuentes, RJ., Lou, BX., Pipas, JM., Gerhardt, J., Rigell, CJ., Fanning, E. Ataxia telangiectasia-mutated damage-signaling kinase- and proteasome-dependent destruction of Mre11-Rad50-Nbs1 subunits in Simian virus 40-infected primate cells. J. Virol. 82 (2008) 5316–28

25. Ali, SH., Kasper, JS., Arai, T., DeCaprio, JA. Cul7/p185/p193 binding to simian virus 40 large T antigen has a role in cellular transformation. J. Virol. 78 (2004) 2749–57

26. Kasper, JS., Kuwabara, H., Arai, T., Ali, SH., DeCaprio, JA. Simian virus 40 large T antigen's association with the CUL7 SCF complex contributes to cellular transformation. J. Virol. 79 (2005) 11685–92

27. Zalvide, J., DeCaprio, J a. Role of pRb-related proteins in simian virus 40 large-T-antigen-mediated transformation. Mol. Cell. Biol. 15 (1995) 5800–10

28. Hein, J., Boichuk, S., Wu, J., Cheng, Y., Freire, R., Jat, PS., Roberts, TM., Gjoerup, O V. Simian virus 40 large T antigen disrupts genome integrity and activates a DNA damage response via Bub1 binding. J. Virol. 83 (2009) 117–27

29. Kierstead, TD., Tevethia, MJ. Association of p53 binding and immortalization of primary C57BL/6 mouse embryo fibroblasts by using simian virus 40 T-antigen mutants bearing internal overlapping deletion mutations. J. Virol. 67 (1993) 1817–29

30. Ahuja, D., Rathi, A V., Greer, AE., Chen, XS., Pipas, JM. A structure-guided mutational analysis of simian virus 40 large T antigen: identification of surface residues required for viral replication and transformation. J. Virol. 83 (2009) 8781–8

31. Welcker, M., Clurman, BE. The SV40 large T antigen contains a decoy phosphodegron that mediates its interactions with Fbw7/hCdc4. J. Biol. Chem. 280 (2005) 7654–8

32. Schneider, J., Fanning, E. Mutations in the phosphorylation sites of simian virus 40 (SV40) T antigen alter its origin DNA-binding specificity for sites I or II and affect SV40 DNA replication activity. J. Virol. 62 (1988) 1598–605

33. Rose, PE., Schaffhausen, BS. Zinc-binding and protein-protein interactions mediated by the polyomavirus large T antigen zinc finger. J. Virol. 69 (1995) 2842–9

34. Ahuja, D., Sáenz-Robles, MT., Pipas, JM. SV40 large T antigen targets multiple cellular pathways to elicit cellular transformation. Oncogene 24 (2005) 7729–45

35. Hurford, RK., Cobrinik, D., Lee, MH., Dyson, N. pRB and p107/p130 are required for the regulated expression of different sets of E2F responsive genes. Genes Dev. 11 (1997) 1447–63

36. Dyson, N. The regulation of E2F by pRB-family proteins. Genes Dev. 12 (1998) 2245–2262

37. May, P., May, E. Twenty years of p53 research: structural and functional aspects of the p53 protein. Oncogene 18 (1999) 7621–36

38. Moll, UM., Petrenko, O. The MDM2-p53 interaction. Mol. Cancer Res. 1 (2003) 1001–8

39. Fuchs, SY., Adler, V., Buschmann, T., Wu, X., Ronai, Z. Mdm2 association with p53 targets its ubiquitination. Oncogene 17 (1998) 2543–7

40. Beckerman, R., Prives, C. Transcriptional regulation by p53. Cold Spring Harb. Perspect. Biol. 2 (2010) a000935

41. Tsai, SC., Pasumarthi, KB., Pajak, L., Franklin, M., Patton, B., Wang, H., Henzel, WJ., Stults, JT., Field, LJ. Simian virus 40 large T antigen binds a novel Bcl-2 homology domain 3-containing proapoptosis protein in the cytoplasm. J. Biol. Chem. 275 (2000) 3239–46

42. Kohrman, DC., Imperiale, MJ. Simian virus 40 large T antigen stably complexes with a 185-kilodalton host protein. J. Virol. 66 (1992) 1752–60

43. Pickart, CM. Mechanisms underlying ubiquitination. Annu. Rev. Biochem. 70 (2001) 503–33

44. Hershko, a., Ciechanover, A. The ubiquitin system. Annu. Rev. Biochem. 67 (1998) 425–79

45. Chen, ZJ., Sun, LJ. Nonproteolytic functions of ubiquitin in cell signaling. Mol. Cell 33 (2009) 275–86

46. Haglund, K., Sigismund, S., Polo, S., Szymkiewicz, I., Di Fiore, PP., Dikic, I. Multiple monoubiquitination of RTKs is sufficient for their endocytosis and degradation. Nat. Cell Biol. 5 (2003) 461–6

47. Komander, D. The emerging complexity of protein ubiquitination. Biochem. Soc. Trans. 37 (2009) 937–53

48. Sarikas, A., Hartmann, T., Pan, Z-Q. The cullin protein family. Genome Biol. 12 (2011) 220

49. Ardley, HC., Robinson, PA. E3 ubiquitin ligases. Essays Biochem. 41 (2005) 15–30

50. Borden, KL., Freemont, PS. The RING finger domain: a recent example of a sequence-structure family. Curr. Opin. Struct. Biol. 6 (1996) 395–401

51. Hatakeyama, S., Nakayama, KI. U-box proteins as a new family of ubiquitin ligases. Biochem. Biophys. Res. Commun. 302 (2003) 635–45

52. Li, W., Bengtson, MH., Ulbrich, A., Matsuda, A., Reddy, VA., Orth, A., Chanda, SK., Batalov, S. Genome-Wide and Functional Annotation of Human E3 Ubiquitin Ligases Identifies MULAN , a Mitochondrial E3 that Regulates the Organelle ' s Dynamics and Signaling. Genome (2008)

53. Skowyra, D., Craig, KL., Tyers, M., Elledge, SJ., Harper, JW. F-box proteins are receptors that recruit phosphorylated substrates to the SCF ubiquitin-ligase complex. Cell 91 (1997) 209–19

54. Feldman, RM., Correll, CC., Kaplan, KB., Deshaies, RJ. A complex of Cdc4p, Skp1p, and Cdc53p/cullin catalyzes ubiquitination of the phosphorylated CDK inhibitor Sic1p. Cell 91 (1997) 221–30

55. Nikolaev, AY., Li, M., Puskas, N., Qin, J., Gu, W. Parc: a cytoplasmic anchor for p53. Cell 112 (2003) 29–40

56. Zheng, N., Schulman, BA., Song, L., Miller, JJ., Jeffrey, PD., Wang, P., Chu, C., Koepp, DM., Elledge, SJ., Pagano, M., Conaway, RC., Conaway, JW., Harper, JW., Pavletich, NP. Structure of the Cul1-Rbx1-Skp1-F boxSkp2 SCF ubiquitin ligase complex. Nature 416 (2002) 703–9

57. Pan, Z-Q., Kentsis, A., Dias, DC., Yamoah, K., Wu, K. Nedd8 on cullin: building an expressway to protein destruction. Oncogene 23 (2004) 1985–97

58. Petroski, MD., Deshaies, RJ. Function and regulation of cullin-RING ubiquitin ligases. Nat. Rev. Mol. Cell Biol. 6 (2005) 9–20

59. Duda, DM., Borg, L a., Scott, DC., Hunt, HW., Hammel, M., Schulman, B a. Structural insights into NEDD8 activation of cullin-RING ligases: conformational control of conjugation. Cell 134 (2008) 995–1006

60. Yamoah, K., Oashi, T., Sarikas, A., Gazdoiu, S., Osman, R., Pan, Z-Q. Autoinhibitory regulation of SCF-mediated ubiquitination by human cullin 1's C-terminal tail. Proc. Natl. Acad. Sci. U. S. A. 105 (2008) 12230–5

61. Lyapina, S., Cope, G., Shevchenko, a., Serino, G., Tsuge, T., Zhou, C., Wolf, D a., Wei, N., Deshaies, RJ. Promotion of NEDD-CUL1 conjugate cleavage by COP9 signalosome. Science 292 (2001) 1382–5

62. Goldenberg, SJ., Cascio, TC., Shumway, SD., Garbutt, KC., Liu, J., Xiong, Y., Zheng, N. Structure of the Cand1-Cul1-Roc1 complex reveals regulatory mechanisms for the assembly of the multisubunit cullin-dependent ubiquitin ligases. Cell 119 (2004) 517–28

63. Carrano, a C., Eytan, E., Hershko, a., Pagano, M. SKP2 is required for ubiquitin-mediated degradation of the CDK inhibitor p27. Nat. Cell Biol. 1 (1999) 193–9

64. Galan, JM., Peter, M. Ubiquitin-dependent degradation of multiple F-box proteins by an autocatalytic mechanism. Proc. Natl. Acad. Sci. U. S. A. 96 (1999) 9124–9

65. Skaar, JR., Pagan, JK., Pagano, M. Mechanisms and function of substrate recruitment by F-box proteins. Nat. Rev. Mol. Cell Biol. (2013)

66. Dias, DC., Dolios, G., Wang, R., Pan, Z. CUL7: A DOC domain-containing cullin selectively binds Skp1.Fbx29 to form an SCF-like complex. Proc. Natl. Acad. Sci. U. S. A. 99 (2002) 16601–6

67. Kasper, JS., Arai, T., DeCaprio, JA. A novel p53-binding domain in CUL7. Biochem. Biophys. Res. Commun. 348 (2006) 132–8

68. Kaustov, L., Lukin, J., Lemak, A., Duan, S., Ho, M., Doherty, R., Penn, LZ., Arrowsmith, CH. The conserved CPH domains of Cul7 and PARC are protein-protein interaction modules that bind the tetramerization domain of p53. J. Biol. Chem. 282 (2007) 11300–7

69. Arai, T., Kasper, JS., Skaar, JR., Ali, SH., Takahashi, C., DeCaprio, J a. Targeted disruption of p185/Cul7 gene results in abnormal vascular morphogenesis. Proc. Natl. Acad. Sci. U. S. A. 100 (2003) 9855–60

70. Litterman, N., Ikeuchi, Y., Gallardo, G., O'Connell, BC., Sowa, ME., Gygi, SP., Harper, JW., Bonni, A. An OBSL1-Cul7 Ubiquitin Ligase Signaling Mechanism Regulates Golgi Morphology and Dendrite Patterning. PLoS Biol. 9 (2011) e1001060

71. Skaar, JR., Arai, T., DeCaprio, JA. Dimerization of CUL7 and PARC is not required for all CUL7 functions and mouse development. Mol. Cell. Biol. 25 (2005) 5579–89

72. Andrews, P., He, YJ., Xiong, Y. Cytoplasmic localized ubiquitin ligase cullin 7 binds to p53 and promotes cell growth by antagonizing p53 function. Oncogene 25 (2006) 4534–48

73. Tron, AE., Arai, T., Duda, DM., Kuwabara, H., Olszewski, JL., Fujiwara, Y., Bahamon, BN., Signoretti, S., Schulman, B a., Decaprio, J a. The Glomuvenous Malformation Protein Glomulin Binds Rbx1 and Regulates Cullin RING Ligase-Mediated Turnover of Fbw7. Mol. Cell 46 (2012) 67–78

74. Duda, DM., Olszewski, JL., Tron, AE., Hammel, M., Lambert, LJ., Waddell, MB., Mittag, T., Decaprio, JA., Schulman, BA. Structure of a Glomulin-RBX1-CUL1 Complex: Inhibition of a RING E3 Ligase through Masking of Its E2-Binding Surface. Mol. Cell (2012) 1–12

75. Skaar, JR., Florens, L., Tsutsumi, T., Arai, T., Tron, A., Swanson, SK., Washburn, MP., Decaprio, JA., Skaar., Florens., Arai., Tron., Washburn. PARC and CUL7 form atypical cullin RING ligase complexes. Cancer Res. 67 (2007) 2006–14

76. Okabe, H., Lee, S-H., Phuchareon, J., Albertson, DG., McCormick, F., Tetsu, O. A critical role for FBXW8 and MAPK in cyclin D1 degradation and cancer cell proliferation. PLoS One 1 (2006) e128

77. Kong, C., Samovski, D., Srikanth, P., Wainszelbaum, MJ., Charron, AJ., Liu, J., Lange, JJ., Chen, P-I., Pan, Z-Q., Su, X., Stahl, PD. Ubiquitination and Degradation of the Hominoid-Specific Oncoprotein TBC1D3 Is Mediated by CUL7 E3 Ligase. PLoS One 7 (2012) e46485

78. Wang, H., Chen, Y., Lin, P., Li, L., Zhou, G., Liu, G., Logsdon, C., Jin, J., Abbruzzese, JL., Tan, T-H. The CUL7/F-box and WD Repeat Domain Containing 8 (CUL7/Fbxw8) Ubiquitin Ligase Promotes Degradation of Hematopoietic Progenitor Kinase 1. J. Biol. Chem. 8 (2013) 0–20

79. Xu, X., Sarikas, A., Dias-Santagata, DC., Dolios, G., Lafontant, PJ., Tsai, S., Zhu, W., Nakajima, H., Nakajima, HO., Field, LJ., Wang, R., Pan, Z. The CUL7 E3 ubiquitin ligase targets insulin receptor substrate 1 for ubiquitin-dependent degradation. Mol. Cell 30 (2008) 403–14

80. Zhang, W., Wang, Q., Song, P., Zou, M. Liver Kinase B1 Is Required for White Adipose Tissue Growth and Differentiation. Diabetes (2013) 1–39

81. Tsutsumi, T., Kuwabara, H., Arai, T., Xiao, Y., Decaprio, JA. Disruption of the Fbxw8 gene results in pre- and postnatal growth retardation in mice. Mol. Cell. Biol. 28 (2008) 743–51

82. Huber, C., Dias-Santagata, D., Glaser, A., O'Sullivan, J., Brauner, R., Wu, K., Xu, X., Pearce, K., Wang, R., Uzielli, MLG., Dagoneau, N., Chemaitilly, W., Superti-Furga, A., Dos Santos, H., Mégarbané, A., Morin, G., Gillessen-Kaesbach, G., Hennekam, R., Van der Burgt, I., Black, GCM., Clayton, PE., Read, A., Le Merrer, M., Scambler, PJ., Munnich, A., Pan, ZQ., Winter, R., Cormier-Daire, V. Identification of mutations in CUL7 in 3-M syndrome. Nat. Genet. 37 (2005) 1119–24

83. Maksimova, N., Hara, K., Miyashia, A., Nikolaeva, I., Shiga, A., Nogovicina, A., Sukhomyasova, A., Argunov, V., Shvedova, A., Ikeuchi, T., Nishizawa, M., Kuwano, R., Onodera, O. Clinical, molecular and histopathological features of short stature syndrome with novel CUL7 mutation in Yakuts: new population isolate in Asia. J. Med. Genet. 44 (2007) 772–8

84. Lee, YH., White, MF. Insulin receptor substrate proteins and diabetes. Arch. Pharm. Res. 27 (2004) 361–70

85. Kim, SJ., Destefano, MA., Oh, WJ., Wu, C., Vega-Cotto, NM., Finlan, M., Liu, D., Su, B., Jacinto, E. mTOR Complex 2 Regulates Proper Turnover of Insulin Receptor Substrate-1 via the Ubiquitin Ligase Subunit Fbw8. Mol. Cell 639 (2012) 1–13

86. Xu, X., Keshwani, M., Meyer, K., Sarikas, A., Taylor, S., Pan, Z-Q. Identification of the degradation determinants of insulin receptor substrate 1 for signaling cullin-RING E3 ubiquitin ligase 7-mediated ubiquitination. J. Biol. Chem. 287 (2012) 40758–66

87. Destefano, MA., Jacinto, E. Regulation of insulin receptor substrate-1 by mTORC2 (mammalian target of rapamycin complex 2). Biochem. Soc. Trans. 41 (2013) 896–901

88. Wainszelbaum, MJ., Liu, J., Kong, C., Srikanth, P., Samovski, D., Su, X., Stahl, PD. TBC1D3, a hominoid-specific gene, delays IRS-1 degradation and promotes insulin signaling by modulating p70 S6 kinase activity. PLoS One 7 (2012) e31225

89. Dearth, RK., Cui, X., Kim, H-J., Kuiatse, I., Lawrence, N a., Zhang, X., Divisova, J., Britton, OL., Mohsin, S., Allred, DC., Hadsell, DL., Lee, A V. Mammary tumorigenesis and metastasis caused by overexpression of insulin receptor substrate 1 (IRS-1) or IRS-2. Mol. Cell. Biol. 26 (2006) 9302–14

90. Hennessy, BT., Smith, DL., Ram, PT., Lu, Y., Mills, GB. Exploiting the PI3K/AKT pathway for cancer drug discovery. Nat. Rev. Drug Discov. 4 (2005) 988–1004

91. Roberts, PJ., Der, CJ. Targeting the Raf-MEK-ERK mitogen-activated protein kinase cascade for the treatment of cancer. Oncogene 26 (2007) 3291–310

92. Haas-Kogan, D., Shalev, N., Wong, M., Mills, G., Yount, G., Stokoe, D. Protein kinase B (PKB/Akt) activity is elevated in glioblastoma cells due to mutation of the tumor suppressor PTEN/MMAC. Curr. Biol. 8 (1998) 1195–8

93. Johnson, GL., Lapadat, R. Mitogen-activated protein kinase pathways mediated by ERK, JNK, and p38 protein kinases. Science 298 (2002) 1911–2

94. Cantley, LC., Neel, BG. New insights into tumor suppression: PTEN suppresses tumor formation by restraining the phosphoinositide 3-kinase/AKT pathway. Proc. Natl. Acad. Sci. U. S. A. 96 (1999) 4240–5

95. Davies, H., Bignell, GR., Cox, C., Stephens, P., Edkins, S., Clegg, S., Teague, J., Woffendin, H., Garnett, MJ., Bottomley, W., Davis, N., Dicks, E., Ewing, R., Floyd, Y., Gray, K., Hall, S., Hawes, R., Hughes, J., Kosmidou, V., Menzies, A., Mould, C., Parker, A., Stevens, C., Watt, S., Hooper, S., Wilson, R., Jayatilake, H., Gusterson, BA., Cooper, C., Shipley, J., Hargrave, D., Pritchard-Jones, K., Maitland, N., Chenevix-Trench, G., Riggins, G., Riggins, GJ., Bigner, DD., Palmieri, G., Cossu, A., Flanagan, A., Nicholson, A., Ho, JWC., Leung, SY., Yuen, ST., Weber, BL., Seigler, HF., Darrow, TL,. Paterson, H., Marais, R., Marshall, CJ., Wooster, R., Stratton, MR., Futreal, PA. Mutations of the BRAF gene in human cancer. Nature 417 (2002) 949–54

96. Robinson, MJ., Cobb, MH. Mitogen-activated protein kinase pathways. Curr. Opin. Cell Biol. 9 (1997) 180–6

97. Pratilas, CA., Xing, F., Solit, DB. Targeting oncogenic BRAF in human cancer. Curr. Top. Microbiol. Immunol. 355 (2012) 83–98

98. Brose, MS., Volpe, P., Feldman, M., Kumar, M., Rishi, I., Gerrero, R., Einhorn, E., Herlyn, M., Minna, J., Nicholson, A., Roth, JA., Albelda, SM., Davies, H., Cox, C., Brignell, G., Stephens, P., Futreal, PA., Wooster, R., Stratton, MR., Weber, BL. BRAF and RAS mutations in human lung cancer and melanoma. Cancer Res. 62 (2002) 6997–7000

99. Steelman, LS., Chappell, WH., Abrams, SL., Kempf, RC., Long, J., Laidler, P., Mijatovic, S., Maksimovic-Ivanic, D., Stivala, F., Mazzarino, MC., Donia, M., Fagone, P., Malaponte, G., Nicoletti, F., Libra, M., Milella, M., Tafuri, A., Bonati, A., Bäsecke, J., Cocco, L., Evangelisti, C., Martelli, AM., Montalto, G., Cervello, M., McCubrey, JA. Roles of the Raf/MEK/ERK and PI3K/PTEN/Akt/mTOR pathways in controlling growth and sensitivity to therapy-implications for cancer and aging. Aging (Albany. NY). 3 (2011) 192–222

100. Chang, Q., Li, Y., White, MF., Fletcher, JA., Xiao, S. Constitutive activation of insulin receptor substrate 1 is a frequent event in human tumors: therapeutic implications. Cancer Res. 62 (2002) 6035–8

101. Nehrbass, D., Klimek, F., Bannasch, P. Overexpression of insulin receptor substrate-1 emerges early in hepatocarcinogenesis and elicits preneoplastic hepatic glycogenosis. Am. J. Pathol. 152 (1998) 341–5

102. Bergmann, U., Funatomi, H., Kornmann, M., Beger, HG., Korc, M. Increased expression of insulin receptor substrate-1 in human pancreatic cancer. Biochem. Biophys. Res. Commun. 220 (1996) 886–90

103. Porcu, P., Ferber, A., Pietrzkowski, Z., Roberts, CT., Adamo, M., LeRoith, D., Baserga, R. The growth-stimulatory effect of simian virus 40 T antigen requires the interaction of insulinlike growth factor 1 with its receptor. Mol. Cell. Biol. 12 (1992) 5069–77

104. Sell, C., Rubini, M., Rubin, R., Liu, JP., Efstratiadis, a., Baserga, R. Simian virus 40 large tumor antigen is unable to transform mouse embryonic fibroblasts lacking type 1 insulin-like growth factor receptor. Proc. Natl. Acad. Sci. U. S. A. 90 (1993) 11217–21

105. DeAngelis, T., Chen, J., Wu, A., Prisco, M., Baserga, R. Transformation by the simian virus 40 T antigen is regulated by IGF-I receptor and IRS-1 signaling. Oncogene 25 (2006) 32–42

106. Fei, ZL., D'Ambrosio, C., Li, S., Surmacz, E., Baserga, R. Association of insulin receptor substrate 1 with simian virus 40 large T antigen. Mol. Cell. Biol. 15 (1995) 4232–39

107. D'Ambrosio, C., Keller, SR., Morrione, A., Lienhard, GE., Baserga, R., Surmacz, E. Transforming potential of the insulin receptor substrate 1. Cell Growth Differ. 6 (1995) 557–62

108. Wu, A., Chen, J., Baserga, R. The role of insulin receptor substrate-1 in the oncogenicity of simian virus 40 T antigen. Cell Cycle 7 (2008) 1999–2002

109. Reiss, K., Del Valle, L., Lassak, A., Trojanek, J. Nuclear IRS-1 and cancer. J. Cell. Physiol. (2011) 2992–3000

110. Thompson, J., Epting, T., Schwarzkopf, G., Singhofen, A., Eades-Perner, a M., van Der Putten, H., Zimmermann, W. A transgenic mouse line that develops early-onset invasive gastric carcinoma provides a model for carcinoembryonic antigen-targeted tumor therapy. Int. J. Cancer 86 (2000) 863–9

111. Mastrangelo, IA., Hough, P V., Wall, JS., Dodson, M., Dean, FB., Hurwitz, J. ATP-dependent assembly of double hexamers of SV40 T antigen at the viral origin of DNA replication. Nature 338 (1989) 658–662

112. Hartmann, T., Xu, X., Kronast, M., Muehlich, S., Meyer, K., Zimmermann, W., Hurwitz, J., Pan, Z-Q., Engelhardt, S., Sarikas, A. Inhibition of Cullin-RING E3 ubiquitin ligase 7 by simian virus 40 large T antigen. Proc. Natl. Acad. Sci. U. S. A. (2014) in press

113. Yu, Y., Alwine, JC. Interaction between simian virus 40 large T antigen and insulin receptor substrate 1 is disrupted by the K1 mutation, resulting in the loss of large T antigen-mediated phosphorylation of Akt. J. Virol. 82 (2008) 4521–6

114. Roskoski, R. ERK1/2 MAP kinases: structure, function, and regulation. Pharmacol. Res. 66 (2012) 105–43

115. Ihler, F., Vetter, EV., Pan, J., Kammerer, R., Debey-Pascher, S., Schultze, JL., Zimmermann, W., Enders, G. Expression of a neuroendocrine gene signature in gastric tumor cells from CEA 424-SV40 large T antigen-transgenic mice depends on SV40 large T antigen. PLoS One 7 (2012) e29846

116. Cheng, J., DeCaprio, JA., Fluck, MM., Schaffhausen, BS. Cellular transformation by Simian Virus 40 and Murine Polyoma Virus T antigens. Semin. Cancer Biol. 19 (2009) 218–28

117. Sachsenmeier, KF., Pipas, JM. Inhibition of Rb and p53 is insufficient for SV40 T-antigen transformation. Virology 283 (2001) 40–8

118. Scheufele, F., Wolf, B., Kruse, M., Hartmann, T., Lempart, J., Mühlich, S., Pfeiffer, AFH., Field, LJ., Charron, MJ., Pan, Z-Q., Engelhardt, S., Sarikas, A. Evidence for a regulatory role of Cullin-RING E3 ubiquitin ligase 7 in insulin signaling. Cell. Signal. 26 (2013) 233–239

119. Zhande, R., Mitchell, JJ., Wu, J., Sun, XJ. Molecular mechanism of insulin-induced degradation of insulin receptor substrate 1. Mol. Cell. Biol. 22 (2002) 1016–26

120. Haruta, T., Uno, T., Kawahara, J., Takano, A., Egawa, K., Sharma, PM., Olefsky, JM., Kobayashi, M. A rapamycin-sensitive pathway down-regulates insulin signaling via phosphorylation and proteasomal degradation of insulin receptor substrate-1. Mol. Endocrinol. 14 (2000) 783–94

121. Lee, a V., Gooch, JL., Oesterreich, S., Guler, RL., Yee, D. Insulin-like growth factor I-induced degradation of insulin receptor substrate 1 is mediated by the 26S proteasome and blocked by phosphatidylinositol 3'-kinase inhibition. Mol. Cell. Biol. 20 (2000) 1489–96

122. Valentinis, B., Navarro, M., Zanocco-Marani, T., Edmonds, P., McCormick, J., Morrione, a., Sacchi, a., Romano, G., Reiss, K., Baserga, R. Insulin receptor substrate-1, p70S6K, and cell size in transformation and differentiation of hemopoietic cells. J. Biol. Chem. 275 (2000) 25451–9

123. Cristofanelli, B., Valentinis, B., Soddu, S., Rizzo, MG., Marchetti, a., Bossi, G., Morena, a R., Dews, M., Baserga, R., Sacchi, a. Cooperative transformation of 32D cells by the combined expression of IRS-1 and V-Ha-Ras. Oncogene 19 (2000) 3245–55

124. Yu, Y., Alwine, JC. Human cytomegalovirus major immediate-early proteins and simian virus 40 large T antigen can inhibit apoptosis through activation of the phosphatidylinositide 3'-OH kinase pathway and the cellular kinase Akt. J. Virol. 76 (2002) 3731–8

125. Manning, BD., Logsdon, MN., Lipovsky, AI., Abbott, D., Kwiatkowski, DJ., Cantley, LC. Feedback inhibition of Akt signaling limits the growth of tumors lacking Tsc2. Genes Dev. 19 (2005) 1773–8

# 7 Publications

- Sarikas, A., **Hartmann, T.**, Pan, Z-Q. The cullin protein family. Genome Biol. 12 (2011) 220.

- Scheufele, F., Wolf, B., Kruse, M., **Hartmann, T.**, Lempart, J., Mühlich, S., Pfeiffer, AFH., Field, LJ., Charron, MJ., Pan, Z-Q., Engelhardt, S., Sarikas, A. Evidence for a regulatory role of Cullin-RING E3 ubiquitin ligase 7 in insulin signaling. Cell. Signal. 26 (2013) 233–239.

- **Hartmann T.**, Xu X., Kronast M., Mühlich S., Meyer M., Zimmermann W., Hurwitz J., Pan Z-Q., Engelhardt S., Sarikas A. Inhibition of Cullin-RING E3 ubiquitin ligase 7 by simian virus 40 large T antigen. PNAS (2014) in press.

# 8 Congress contributions

- **Hartmann T.**, Antonio S. Role of the Cullin7 E3 ubiquitin ligase in oncogenic transformation by Simian Virus 40 large T-antigen. EMBO Ubiquitin and SUMO Workshop, Split, Croatia (2010).

- **Hartmann T.**, Engelhardt S., Antonio S. Inhibition of the Cullin7 E3 ubiquitin ligase by the viral oncoprotein SV40 large T-antigen. 77$^{th}$ annual meeting of the Deutsche Gesellschaft für experimentelle und klinische Pharmakologie und Toxikologie (DGPT) (2011).

- **Hartmann T.**, Engelhardt S., Antonio S. Inhibition of the Cullin7 E3 ubiquitin ligase by the viral oncoprotein SV40 large T-antigen. 79$^{th}$ annual meeting of the Deutsche Gesellschaft für experimentelle und klinische Pharmakologie und Toxikologie (DGPT) (2013).

# 9 Appendix

## 9.1 Abbreviations

| | | | |
|---|---|---|---|
| aa | Amino acid | LKB1 | Liver kinase B1 |
| ATP | Adenosintriphosphate | LT-antigen/LT | Large T-antigen |
| AU | Arbitrary units | ΔLT-antigen /ΔLT | Δ69-83 large T-antigen |
| BKV | BK polyomavirus | MCV | Merkel cell polyomavirus |
| bp | Base pairs | MEF | Mouse embryonic fibroblast |
| BTB | Bric-a-brac, Tramtrack, Broad-complex | MRN | MRE11, RAD50 and NBS1 complex |
| C-terminus | Carboxyl terminus | mRNA | Messanger RNA |
| CAND1 | Cullin-associated and neddylation-dissociated protein 1 | N-terminus | Amino terminus |
| Cdk | Cycline dependent kinase | Na3VO4 | Sodium orthovanadate |
| cDNA | Complementary DNA | NaF | Sodium fluoride |
| CEA | Carcinoembryonic antigen | $NaN_3$ | Sodium azide |
| CH | Cullin homology domain | NEDD8 | Neural precursor cell expressed, developmentally down-regulated 8 |
| Ci | Curie | OBD | Origin binding domain |
| CIP | Calf intestinal phosphoatase | ori | Origin of replication |
| CR1-3 | Cullin repeat 1-3 | P | Phospho |
| CRL(1-7) | Cullin RING E3 ubiquitin ligase (1-7) | PARC | p53-associated parkin-like cytoplasmatic protein |
| CSN | Cop9 signalosome | PBS | Phosphate buffered saline |
| Ct | Cycle treshold | PCR | Polymerase chain reaction |
| ctr | Control | PE | early promoter |
| CUL7 | Cullin 7 | PI3K | Phosphoinositide 3-kinase |
| DAPI | 4´,6´-diamino-2-phenylindole | PL | late promoter |
| DCAF | DDB1-CUL4 associated factor | PP2A | Protein phosphatase A |
| DDB1 | DNA damage-binding protein 1 | pRB | Retinoblastoma protein |
| ddH2O | Double distilled water | qRT-PCR | Quantitative real-time PCR |
| DDR | DNA damage response | Rbx1/2 | RING-box protein 1/2 |
| DM | Dulbecco's modified eagle´s medium | rcf | Relative centrifugal force |
| DMSO | Dimethyl sulfoxide | RING | Really interesting new gene |

| | | | |
|---|---|---|---|
| DNA | Desoxyribonucleic acid | RNA | Ribonucleic acid |
| dNTP | Desoxyribonucleotide triphosphates | RNase | Ribonuclease |
| ds | Double-stranded | ROC1/2 | Regulator of Cullins 1/2 |
| DTT | Dithiothreitol | RPA | Replication protein A |
| E.coli | Escherichia coli | rpm | Rounds per minute |
| E1 | Ubiquitin-activating enzyme | RT | Room temperature |
| E2 | Ubiquitin-conjugating enzyme | SCF | Skp1, CUL1, F-box complex |
| E3 | Ubiquitin ligase | SDS | Sodiumdodecylsulfate |
| EDTA | Ethylenediaminetetraacetic acid | SDS-PAGE | Sodiumdodecylsulfate-polyacrylamid gel electrophoresis |
| EV | Empty vector | SEM | Standard error of mean |
| FCS | Fetal calf serum | siRNA | Short interfering RNA |
| Fig. | Figure | Skp1 | S-phase kinase-associated protein 1 |
| HE | Hematoxylin und eosin | SOCS | Suppressor of cytokine signaling |
| HECT | Homologous to E6-associated protein C-terminus | ss | Single-stranded |
| HPV | Human papillomavirus | ST-antigen | Small T-antigen |
| HR | Host range domain | SV40 | Simian virus 40 |
| HRP | Horseradish peroxidase | TAE | Tris acetate buffer |
| IBR | in-between RING | TCF | ternary complex factor |
| IEG | immediate early genes | Topo I | Topoisomerase I |
| IGF-1 | Insulin-like growth factor 1 | TSV | Trichodysplasia spinulosa-associated polyomavirus |
| IGF-1R | IGF-1 receptor | Ub | Ubiquitin |
| IHC | Immunohistochemie | UPS | Ubiquitin-proteasome system |
| IP | Immunoprecipitation | UV | Ultraviolet |
| IRS1 | Insulin receptor substrate 1 | VHL | von Hippel-Lindau |
| JCV | JC polyomavirus | v/v | % volume per volume |
| kb | Kilobase | w/v | % weight per volume |
| kDa | Kilodalton | WCL | Whole cell lysate |
| LB medium | Lysogeny broth medium | Zn | Zinc |

## 9.2 Acknowledgements

I would like to express my special appreciation and thanks to my advisors Professor Dr. Dr. Stefan Engelhardt and Dr. Antonio Sarikas, you have been tremendous mentors for me. I would like to thank you both for encouraging my research and for allowing me to grow as a research scientist. I would also like to thank Professor Dr. Claus Schwechheimer (TUM, Freising, Germany) for the scientific discussion of my work and for being part of my Ph.D. committee.

I also would like to thank our collaboration partners Prof. Dr. Zhen-Qiang Pan (New York, USA), Prof. Dr. Wolfgang Zimmermann (LMU, Munich, Germany) and Dr. Susanne Muehlich (LMU, Munich, Germany). Furthermore I would like to thank Prof. Dr. James DeCaprio (Boston, USA), Prof. Dr. Azad Bonni (Boston, USA) and Dr. Per Sonne Holm (Munich, Germany) for providing plasmids and cell lines.

Especially I would like to thank all current and former lab members of the Institute of Pharmacology and Toxicology for their helpfulness and support in the daily lab work and the wonderful atmosphere. All of you have been there to support me in scientific question and helped me to collected data for my Ph.D. thesis. Also many thanks for the great eventful times we had beside our daily lab work.

Finally, special thanks go to my family and friends. You always supported me in any situation and provided distraction from the daily work when it was necessary.